

Derivation and thermodynamically consistent coupling of a Debye-Hückel type energy to a steric electrolyte model and application to the apparent molar volume and phase boundaries

Wolfgang Dreyer

Rüdiger Müller
rue.m.sci@gmail.com

February 13, 2025

Abstract

We propose to determine the size parameters of a steric electrolyte model from the experimental data of apparent molar volume obtained from mass density measurements. Thereby, we avoid the difficulties associated with modeling the complex structure of the double layer. To this end, we derive a Debye-Hückel-like model of the electric ion-ion interaction for non-constant dielectric susceptibility, which does not depend on any kind of charging process due to its foundation in the general framework of non-equilibrium electro-thermodynamics. The derivation, however, leads to a novel thermodynamic consistency condition for the temperature dependence of the susceptibility. Due to its contributions to the total pressure, the consistent coupling of this new contribution to the free energy requires subtle modifications in the derivation of the simple mixing model for electrolytes. The coupled model is then applied to the apparent molar volume for various related monovalent salts over a wider range of salt concentrations and temperatures, and classical tests of the electrolyte theory at phase boundaries are investigated.

1 Introduction

Mixing salt in water and observing the change in volume and mass density seems to be one of the simplest experiments imaginable, cf. [RM64]. But even this experiment can reveal shortcomings and limitations of standard continuum models of electrolytes. In particular, frequently used steric Poisson-Boltzmann models, cf. e.g. [KII96, BAO97, KBA07, DGM13], can not be expected to yield meaningful results in predicting mass density or apparent molar volume of electrolytes, despite the fact that they are developed with the goal to handle volume exclusion effects. In principle, the experiment

can be considered as sufficiently explained by the Debye-Hückel theory [DH23a], at least in the limit of strong dilution. Nevertheless, the Debye-Hückel theory is often considered too simplified and, for example, the role of non-constant susceptibility is still actively discussed [VB14, SL15, KMMT18, SLK23]. While classical Debye-Hückel theory is usually considered applicable only for dilute solutions, steric Poisson-Boltzmann like models are designed for concentrated electrolytes. Thus it appears worthwhile to couple both approaches. With the aim of comprehensive and fundamental revision of the modeling within the context of non-equilibrium electro-thermodynamics, the main goals here are:

1. Derivation of a Debye-Hückel-like electric interaction energy that consistently incorporates temperature and concentration dependent susceptibility from the outset.
2. Establishing the non-obvious consistent coupling of the steric simple mixture model with the obtained interaction energy.
3. Incorporating in general incomplete dissociation in order to apply linear material laws for mixtures while still retaining the nonlinear observed behavior.
4. Testing the developed theory over a wider concentration and temperature range using the phenomena of apparent molar volume and phase equilibrium at phase boundaries.

1.1 Some historic background of models

Ideal electrolyte theory. The microscopic concept of dissociation of a salt into ions was introduced by Arrhenius [Arr87] and greatly supported by van't Hoff's observation of the analogy between diluted electrolyte solutions and osmosis at semi-permeable membranes. Thus, in the early electrolyte theory ideality was expressed by the logarithmic chemical potential inherited from the ideal gases and Ostwald's mass action law. The theory relied on incomplete dissociation to account for the Kohlrausch square root law observed in conductivity measurements. However, the classical ideal electrolyte model was not able to explain different experimental data consistently. In particular, when assuming the dissociation degree determined by conductivity measurement, then the Ostwald mass action law was not able to yield a reaction constant, cf.[Red46]. We remark that in light of the non-equilibrium thermodynamic theory, which was only developed decades later, equilibrium quantities like the free energy or chemical potentials should not be determined by non-equilibrium properties like the electrolyte conductivity, cf. e.g. [DGM19]. The classical ideal theory leads on a macroscopic scale to a Boltzmann distribution of ions and where ions do not necessarily have to be point charges, but volume exclusion effects can be neglected due to the

strong dilution assumption and thus there is no mechanism in the model to limit charge accumulation at strongly charged surfaces.

Steric electrolyte models. In the electrochemical double layer, electrolytes are in general concentrated and there is voltage drop over a typically very short distance, giving rise to locally extremely strong electric fields. The standard Poisson-Boltzmann model of ideal electrolytes can adequately account for the action of this electric field on ions but the missing of volume exclusion effects prevent the model to reasonably limit the local boundary layer charge. Therefore, in steric modified Poisson-Boltzmann models a size parameter is added to change the mixing entropy of ideal gases into a lattice gas approach [KII96, BAO97, KBA07]. Extensions of lattice gas models to ions of different size have also been developed, cf. e.g. [CBL⁺07, Li09, LE14] and the review in [ZH18]. Instead of the lattice gas approach, in the very general simple mixture model [DGM13, LGD16, DGM18], the mixing entropy accounts for solvation of ions although formally looking identic to the ideal gas case, and adds an elastic energy contribution to the free energy in order to account for elastic interaction of constituents of finite size. In an incompressible limit of the elastic law, the non-ideality is expressed in a dependence of the chemical potentials on the local pressure the model can be reduced to a lattice gas. An axiomatic derivation of the simple mixture is provided in [BDD23] and it is shown that the incompressible limit requires linear dependence of the volume on the mixtures composition. Steric modified Poisson-Boltzmann models which account for the concentration dependence with linear dielectric decrement are proposed in [BYAP11, HvRL12, NA15, FCBM16] and extended to different ion sizes developed in [GS18, LM22]. For steric models taking into account the dependency of the susceptibility on the strong electric field in the double layer, we refer to [LM22] and references therein.

Debye-Hückel theory. Because the double layer screens outer electric fields from the electrolyte bulk, it leaves in equilibrium the bulk electrolyte free of any electric field and the above models of electrolytes reduce to mixtures of uncharged particles, although the electrolytes consists besides of the solvent of negatively charged anions and positive cations. As a way to take electric ion-ion interactions into account within a homogeneous, macroscopically electroneutral electrolyte, Debye and Hückel introduced in 1923 a mean field model [DH23a]. They determined the electric energy gained by an arbitrary selected ion under the assumptions that: (i.) the surrounding environment can be described in a continuum way and is solely characterized by its constant susceptibility (ii.) the electrolytic environment can be described by Boltzmann distribution and linearization is admissible. Then, the free energy density is deduced analytically by integrating the inner energy density with respect to temperature. By this it was possible to explain

non-ideal behavior at phase boundaries without having to rely on incomplete dissociation. Most important, it was possible to formulate limiting laws for strong dilution, that did not depend on the specific salt, but only on the valency of the ions. The Debye-Hückel theory was rapidly adopted by others and tested in different experimental applications. Deviations from the limit law were found even at moderate salt concentrations, especially for multivalent ions, and an ion-specific behavior of the heat of dilution was observed [GH25, LM29]. For the apparent molar volume, the limit law even predicted the wrong sign of the slope [RM64] and the correct sign was obtained only when the susceptibility depends on the pressure [RR31]. However, a susceptibility depending on temperature is not compatible with the derivation of the free energy in [DH23a]. Debye therefore introduced the thought experiment of a hypothetical charging process [Deb24], which allows non-constant susceptibility, and arrived at the same result as before. Although the justification of the charging process remained somewhat controversial, cf. e.g. [GH25, KMMT18] and the references therein, it is now generally accepted. Already in 1925 Hückel proposed a linear dependence of the susceptibility on the salt concentration and a splitting of energy in ionic and solvation contributions [Hüc25]. In [SL15], the charging process is carried out with non-linear concentration-dependent susceptibility based on experimental data. The splitting of potentials and concentration dependent susceptibility are applied in [VVB10, VB14, VB23] together with a non-primitive model based on molecular simulations. An extended Debye-Hückel theory based on a Poisson–Fermi approach was proposed in [LE15, LE18]. Various modifications and extensions related to the susceptibility and the charging process are reviewed in [KMMT18, SLK23].

The electric ion-ion interaction was also employed in a non-equilibrium context to derive non-ideal ionic conductivity without having to rely on incomplete dissociation. By adding Brownian motion in [Ons27], the square root law of the conductivity by Debye-Hückel [DH23b] was improved and dependence of conductivity on ionic radius was removed. We will not consider the non-equilibrium case further here.

1.2 Aims and scope

In the following, we aim at developing a macroscopic continuum model within the framework of non-equilibrium electro-thermodynamics. The model must consistently couple steric effects of finite volumes with the electrical interaction between ions. Effects originating from the microscopic scale, which are explicitly resolved within the so-called non-primitive models cf. e.g. [VB14], must be taken into account implicitly in the susceptibility. The charging process is avoided in the derivation.

Solvated ions. The first step in modeling is to define the constituents of the mixture, in particular whether solvated ions or just the bare unsolvated ions should be considered as constituents. The application of a solvated radius in the model is rejected in [VB14, VB23] because it might hinder the contact of ions to structural groups or the formation of ion pairs. To the contrary, [Zav01] emphasises the importance of modeling the reduction of free solvent molecules due to solvation since this way already large amounts of the non-ideality of the electrolytes can be removed. Similar ideas can also be found in [RS02] and it is also comparable with a simple mixture model [LGD16, DGM18] but with non-integer solvation numbers applied. In a the simple mixture that we use, size parameters for each of the constituents are needed. While in previous work [LGD16, LM22], solvation numbers and specific volumes were adjusted to data from differential capacitance of the double layer we here want in contrast to deduce specific volumes of possibly solvated ions from much more directly related experiments on the mass density or the apparent molar volume. In particular, adding a solute to the solvent, the solution volume may increase by less than the volume of added solute, or it may even decrease. For example, the volume decreases in aqueous LiF and NaF solutions such that a negative volume would have to be assigned to the bare F^- ion. In contrast, the solvated ion still has a positive volume, although it is less than the volume of the individual solvent molecules in the solvation shell combined.

Incomplete dissociation. At the time of [DH23a], incomplete dissociation on the one hand and electrostatic ion-ion interaction on the other hand, were considered exclusive alternatives to explain non-ideal behavior, c.f. [Red46]. Later, the concept of ion pairing was (re)introduced by Bjerrum [Bje26]. Nowadays, the dominant opinion in the literature, with the exception of [Hey96], is such that while there is ion pairing in weaker electrolytes and in some strong electrolytes at higher concentrations, there is no ion pairing of alkali halides in water, cf. [MH06, MR17]. We include incomplete dissociation in the general model, with the possibility that a-posteriori its relevance in certain applications may prove to be low.

1.3 Outline

We start in Sect. 2 by characterizing the assumptions and stating the electro-thermodynamic framework. In Sect. 3, the axiomatic approach of [BDD23] is slightly modified to derive in Sect. 3.2 and 3.3 a simple mixture model that can be coupled to the Debye-Hückel type free energy contribution which is derived in Sect. 3.4 and 3.5. The full coupled model is then applied to the apparent molar volume related to mass density measurement of aqueous electrolytes in Sect. 4. Concentration and temperature dependence are investigated numerically and a set of ion-specific parameters is deduced for

several related salts. In Sect. 5 the model is tested at phase boundaries through experiments on the vapour pressure reduction and the freezing point depression. We conclude in Sect. 6 with a discussion of the model, its application and remaining open issues.

2 General thermodynamic model

We apply the general electro-thermodynamic model framework based on [dGM84, Mül85] and particularly adapted for electrochemical bulk-surface systems in [DGM18, ML23]. It relies on the exploitation of an entropy principle for the restriction of constitutive quantities like fluxes, stress or reaction rates. A particular ingredient in the entropy principle is the specification of a constitutive function for the entropy density, i.e. the definition of its set of independent variables.

We denote the spatial domain occupied by an electrolyte by $\Omega \subseteq \mathbb{R}^3$ and use index sets \mathcal{I} to refer to the different constituents of the mixture in Ω . Each constituent in Ω has the (atomic) mass m_α , for $\alpha \in \mathcal{I}$, and the net charge $z_\alpha e_0$, where z_α is the charge number of the constituent and e_0 is the elementary charge.

2.1 Assumptions and thermodynamic consistency

We consider the *entropy density* ρs to be a function of the *inner energy density* ρu , the (local) particle number densities per m^3 denoted as n_α for $\alpha \in \mathcal{I}$ and the *vector of polarization* \mathbf{P} as the independent variables that determine the Thermodynamic state in Ω .

Temperature. The constitutive modeling is greatly eased by the introduction of the *temperature* T and the *free energy density* $\rho\psi$ by means the Legendre transformation of the entropy density ρs with respect to the inner energy density ρu , viz.

$$\rho\psi = \rho u - T \rho s, \quad \text{with} \quad \frac{1}{T} = \frac{\partial}{\partial \rho u} \rho s. \quad (1)$$

Then we obtain the consistency conditions

$$\rho s = -\frac{\partial}{\partial T} \rho\psi, \quad \rho u = -T^2 \frac{\partial}{\partial T} \left(\frac{\rho\psi}{T} \right). \quad (2)$$

Assumptions on the electric field.

- in the considered applications, all relevant features of electrochemical system can be well described in the *quasi-electrostatic* limit of Maxwell

equations. Thus, the electromotoric force equals the electric field \mathbf{E} and there exists an *electrostatic potential* φ , such that

$$\mathbf{E} = -\nabla\varphi, \quad [[\varphi]] = \text{const. on intersecting surfaces}, \quad (3)$$

where the constant is frequently chosen as zero.

- The timescale of polarization relaxation in liquid electrolytes is typically in the range of 10^{-8} s (cf. [BHM99]), and therefore orders of magnitude smaller than the relevant observed time scales of the considered application. Thus, we assume quasi-equilibrium of polarization relaxation.
- We assume that the dielectric properties of the liquid electrolyte are reasonably well represented by a scalar susceptibility χ which may be a function of temperature and the electrolyte composition. Since the focus here is not on boundary layers where the electric field strength can be the extremely high, we assume in order to reduce complexity that χ is independent of the electric field \mathbf{E} .

As discussed in [LM22, ML23] these assumptions allow to use the electric field \mathbf{E} instead of \mathbf{P} as an independent variable for the constitutive functions and to relate \mathbf{E} to the the vector of polarization by

$$\mathbf{P} = -\frac{\partial\rho\psi}{\partial\mathbf{E}}, \quad \mathbf{P} = \chi \cdot \varepsilon_0 \mathbf{E}. \quad (4)$$

Thermodynamic consistency. The simple relations (4) suggest to choose for the free energy a constitutive function depending on temperature, the composition of the mixture and the electric field as

$$\rho\psi = \rho\hat{\psi}(T, (n_\alpha)_{\alpha \in \mathcal{I}}) - \chi \frac{\varepsilon_0}{2} |\mathbf{E}|^2. \quad (5)$$

From (1) and (2) we obtain an analogous splitting of the entropy density and the inner energy density as

$$\rho s = -\frac{\partial}{\partial T} \rho\hat{\psi} + \frac{\partial}{\partial T} \chi \frac{\varepsilon_0}{2} |\mathbf{E}|^2 = \rho\hat{s} + \frac{\partial}{\partial T} \chi \frac{\varepsilon_0}{2} |\mathbf{E}|^2, \quad (6a)$$

$$\rho u = -T^2 \frac{\partial}{\partial T} \left(\frac{\rho\hat{\psi}}{T} \right) - T^2 \frac{\partial}{\partial T} \left(\frac{-\chi \frac{\varepsilon_0}{2} |\mathbf{E}|^2}{T} \right) = \rho\hat{u} - \left(\chi - T \frac{\partial}{\partial T} \chi \right) \frac{\varepsilon_0}{2} |\mathbf{E}|^2, \quad (6b)$$

such that $\rho\hat{\psi} = \rho\hat{u} - T\rho\hat{s}$. Moreover, an analogous splitting holds for the chemical potentials, i.e.

$$\mu_\alpha = \frac{\partial\rho\psi}{\partial n_\alpha} = \hat{\mu}_\alpha - \frac{\partial}{\partial n_\alpha} \chi \frac{\varepsilon_0}{2} |\mathbf{E}|^2. \quad (7)$$

By means of a Gibbs-Duhem relation, we introduce a quantity that we refer to as pressure, viz.

$$\begin{aligned} p &:= -\rho\psi + \sum_{\alpha \in \mathcal{I}} n_\alpha \mu \\ &= -\rho\hat{\psi} + \sum_{\alpha \in \mathcal{I}} n_\alpha \hat{\mu}_\alpha + \frac{1}{2}\varepsilon_0 |\mathbf{E}|^2 \left(\chi - \sum_{\alpha \in \mathcal{I}} n_\alpha \frac{\partial}{\partial n_\alpha} \chi \right) = \hat{p} + p^{\text{el}} . \end{aligned} \quad (8)$$

In order to get a correct interpretation of the pressure, p has to be related to the momentum balance.

2.2 Balance equations of charged mixtures

We summarise here the model equations adapted to the above simplifying assumptions, i.e. fast polarisation relaxation. The *total mass density*, the *barycentric velocity* and the *free charge density* are defined as

$$\rho = \sum_{\alpha \in \mathcal{I}} m_\alpha n_\alpha , \quad \mathbf{v} = \sum_{\alpha \in \mathcal{I}} m_\alpha n_\alpha \mathbf{v}_\alpha , \quad n^{\text{F}} = e_0 \sum_{\alpha \in \mathcal{I}} z_\alpha n_\alpha , \quad (9)$$

where \mathbf{v}_α denotes the velocity of constituent $\alpha \in \mathcal{I}$. Within the volume domain Ω the balance equations are for time $t > 0$

$$-\text{div}((1 + \chi)\varepsilon_0 \nabla \varphi) = n^{\text{F}} , \quad (10a)$$

$$\partial_t \rho_\alpha + \text{div}(\rho_\alpha \mathbf{v} + \mathbf{J}_\alpha) = m_\alpha \sum_k \nu_\alpha^k R^k , \quad (10b)$$

$$\partial_t(\rho \mathbf{v}) + \text{div}(\rho \mathbf{v} \otimes \mathbf{v} - \boldsymbol{\sigma}^{\text{visc}}) + \nabla p = \rho \mathbf{f} - n^{\text{F}} \nabla \varphi + (D^2 \varphi) \chi \varepsilon_0 \nabla \varphi , \quad (10c)$$

$$\begin{aligned} \partial_t(\rho u) + \text{div}(\rho u \mathbf{v} + \mathbf{Q}) &= -\mathbf{J}^{\text{F}} \cdot \nabla \varphi + \boldsymbol{\sigma}^{\text{visc}} : \nabla \mathbf{v} - p \text{div}(\mathbf{v}) \\ &\quad + (\partial_t(\chi \varepsilon_0 \nabla \varphi) + (\mathbf{v} \cdot \nabla)(\chi \varepsilon_0 \nabla \varphi)) \cdot \nabla \varphi \end{aligned} \quad (10d)$$

$$+ \chi \varepsilon_0 |\nabla \varphi|^2 \text{div}(\mathbf{v}) ,$$

Each one of the reactions with the reaction rates R^k in (10b) has to conserve mass and charge and not all of the diffusive mass fluxes \mathbf{J}_α are linearly independent. We thus have for the stoichiometric coefficients ν_α^k and for the fluxes the constraints

$$\sum_{\alpha \in \mathcal{I}} m_\alpha \nu_\alpha^k = 0 , \quad \sum_{\alpha \in \mathcal{I}} z_\alpha \nu_\alpha^k = 0 , \quad \sum_{\alpha \in \mathcal{I}} \mathbf{J}_\alpha = 0 , \quad (11)$$

such that one of the partial mass balances (10b) can be replaced by the total mass balance. The right hand side of the momentum balance (10c) contains external body forces $\rho \mathbf{f}$ like gravitational force and in addition Lorentz force and the Kelvin force term $(\nabla \mathbf{E}) \mathbf{P}$. Taking the p^{el} contribution out of the

pressure term ∇p on the left hand side and combining it with the Kelvin force term on the right hand side, we get the Korteweg-Helmholtz force density, cf. [LM22, Sect. 3.2] and references therein. The pressure term and all forces except of the external body force can be moved into the divergence to form the total stress tensor, viz.

$$\partial_t(\rho \mathbf{v}) + \operatorname{div} \left(\rho \mathbf{v} \otimes \mathbf{v} - \left(\boldsymbol{\sigma}^{\text{visc}} - \hat{p} \mathbf{1} - \left(\frac{\varepsilon_0}{2} |\mathbf{E}|^2 + p^{\text{el}} \right) \mathbf{1} + (\varepsilon_0 \mathbf{E} + \mathbf{P}) \otimes \mathbf{E} \right) \right) = \rho \mathbf{f} , \quad (12)$$

where $\mathbf{1}$ denotes the unit tensor. Then, the field independent part of the total stress tensor consists of $-\hat{p}$ on the diagonal and the viscous stress tensor. The free current in (10d) is $\mathbf{J}^{\text{F}} = e_0 \sum_{\alpha \in \mathcal{I}} z_\alpha \mathbf{J}_\alpha$.

Finally the remaining constitutive quantities are determined by the entropy principle. Due to the linear dependence of the fluxes \mathbf{J}_α , one constituent is selected as a reference. Typically the solvent is chosen and we refer here to the chosen constituent by the index $0 \in \mathcal{I}$. The constitutive equations are for each counting index k and $\alpha \in \mathcal{I} \setminus \{0\}$

$$R^k = R_0^k \cdot \left(1 - \exp \left(\frac{A^k}{k_B T} \sum_{\alpha \in \mathcal{I}^\pm} \nu_\alpha^k \mu_\alpha \right) \right) , \quad (13a)$$

$$\mathbf{J}_\alpha = - \sum_{\gamma \in \mathcal{I} \setminus \{0\}} M_{\alpha\gamma} \cdot \left(\nabla \left(\frac{\mu_\gamma}{T} - \frac{\mu_0}{T} \frac{m_\gamma}{m_0} \right) + \frac{e_0}{T} \left(z_\gamma - z_0 \frac{m_\gamma}{m_0} \right) \nabla \varphi \right) , \quad (13b)$$

$$\boldsymbol{\sigma}^{\text{visc}} = \eta_b \operatorname{div}(\mathbf{v}) \mathbf{1} + \eta_s \cdot (\nabla \mathbf{v} + (\nabla \mathbf{v})^T) , \quad (13c)$$

$$\mathbf{Q} = - \frac{\kappa}{T^2} \nabla T . \quad (13d)$$

The phenomenological coefficients satisfy $A^k > 0$, $\kappa > 0$, $(\eta_b + \frac{3}{2}\eta_s) > 0$, $\eta_s > 0$ and $M_{\alpha\gamma}$ form a positive definite matrix. Most relevant is here that the equilibrium condition following from (13a) is the mass action law. Boundary conditions for the system (10) follow from surface balances and the application of an entropy principle on the surface, cf. [DGM18, ML23].

3 Derivation of the constitutive model

3.1 Outline of our strategy

There are typically two distinct regimes of electrolytes in equilibrium where we propose to apply different constitutive equations:

- (BL) *Boundary layers* at domain boundaries or intersecting surfaces. In these layers there is locally a macroscopic charge imbalance, i.e. $n^{\text{F}} \neq 0$. The according strong electric field, that reaches the order of 10^9 V m^{-1} by far dominates the electric interaction of individual ions. Thus, we

can apply above splitting of the constitutive equations (4)_(right), (5)-(8), with a free energy function $\rho\hat{\psi}(T, (n_\alpha)_{\alpha\in\mathcal{I}})$ like it is used for uncharged particles. In particular, we apply a simple mixture model.

(HB) *Homogeneous bulk* domain are shielded from external electric influence by the boundary layers. On a macroscopic scale, the electrolyte thus appears locally electro-neutral, i.e. $n^F = 0$ and the electric field vanishes, viz. $\mathbf{E} = 0$. This reduces the free energy function (4)_(right) to $\rho\psi = \rho\hat{\psi}(T, (n_\alpha)_{\alpha\in\mathcal{I}})$. The missing of dominant macroscopic electric forces now allows some otherwise neglected higher order effects like the electric interaction of ions to become relevant. We thus combine the simple mixture model with a Debye-Hückel like model that takes into account a microscopic electric field in the vicinity of ions and transfers the electric field energy contribution after spatial averaging into a field independent macroscopic one, i.e., we have

$$\rho\hat{\psi}(T, (n_\alpha)_{\alpha\in\mathcal{I}}) = \rho\psi^{\text{sim}}(T, (n_\alpha)_{\alpha\in\mathcal{I}}) + \rho\psi^{\text{D}}(T, (n_\alpha)_{\alpha\in\mathcal{I}}), \quad (14)$$

where $\rho\hat{\psi}^{\text{sim}}$ and $\rho\hat{\psi}^{\text{D}}$ denote the contributions of the simple mixture model and the Debye-Hückel like model, respectively.

A simple mixture for electrolytes, including entropy of mixing, elastic interactions between the constituents and solvation of ions, has been introduced and discussed in [DGM13, LGD16] for the isothermal case and more general in [BDD23]. In the spirit of [BDD23], we will not directly postulate a free energy function, but rather make assumptions on specific heat, pressure, specific energy and specific entropy. Then, we are able to deduce a free energy function compatible with these assumptions. But since we have to expect both $\rho\psi^{\text{sim}}$ and $\rho\psi^{\text{D}}$ in (14) to contribute to the pressure, some subtle differences compared to [BDD23] are necessary here.

The derivation of Debye-Hückel like model consists of two parts: The first part starts the same way as in [DH23a] with selecting an arbitrary individual ion of the mixture and calculating its electric field interaction with the ions in surrounding neighborhood. In the second part, our approach differs from [DH23a] in the way that we base the calculation of the inner energy and entropy on the splitting (6)_(right), which we assume it also applies to the electric field in the vicinity of the ions on the more microscopic scale. This finally allows a direct identification of the macroscopic energy contributions after spatial averaging.

Table 1: Physical constants.

Boltzmann constant	$k_B = 1.380649 \times 10^{-23} \text{ J K}^{-1}$
elementary charge	$e_0 = 1.602176634 \times 10^{-19} \text{ C}$
Avogadro number	$\mathcal{N}_A = 6.02214076 \times 10^{23} \text{ mol}^{-1}$
dielectric constant	$\varepsilon_0 = 8.8541878188 \times 10^{-12} \text{ C V}^{-1} \text{ m}^{-1}$

3.2 Change of variables and representation equations.

The derivation of a free energy is greatly eased by a change of variables. We denote the total number density and its inverse by

$$n = \sum_{\alpha \in \mathcal{I}} n_\alpha, \quad \nu = \frac{1}{n}, \quad (15)$$

respectively, where ν has the dimensions of a volume. Then, we introduce as new variables the mole fractions

$$y_\alpha = \frac{1}{n} n_\alpha = \nu n_\alpha \quad \text{implying the constraint} \quad \sum_{\alpha \in \mathcal{I}} y_\alpha = 1. \quad (16)$$

For abbreviation we set $\mathbf{y} = (y_\alpha)_{\alpha \in \mathcal{I}}$ and introduce $M(\mathbf{y}) = \sum_{\alpha \in \mathcal{I}} m_\alpha y_\alpha$. We consider three different sets of basic variables to cover the state space, viz.

$$(T, (n_\alpha)_{\alpha \in \mathcal{I}}) \longleftrightarrow (T, \nu, \mathbf{y}) \longleftrightarrow (T, p, \mathbf{y}). \quad (17)$$

While the first one of the variable transformations in (17) is most simple, the second one needs a constitutive equation which has not been specified up to now. This is the so-called *thermal equation of state* relating the pressure to the chosen variables. Depending on the chosen variables, this constitutive law is given in the abstract form

$$p = \bar{p}(T, \nu, \mathbf{y}) \longleftrightarrow \nu = \tilde{\nu}(T, p, \mathbf{y}). \quad (18)$$

For a generic quantity f , we denote the function acting on the first set of variables in (17) as $f = \hat{f}(T, (n_\alpha)_{\alpha \in \mathcal{I}})$. Then, we define two new functions,

$$\bar{f}(T, \nu, \mathbf{y}) := \hat{f}(T, \frac{1}{\nu} \mathbf{y}) \quad \text{and} \quad \tilde{f}(T, p, \mathbf{y}) := \hat{f}(T, \tilde{\nu}(T, p, \mathbf{y}), \mathbf{y}). \quad (19)$$

Obviously the thermal equation of state must satisfy the Gibbs-Duhem equation (8) for $\mathbf{E} = 0$. Thus, by using (19) and applying chain rule, we easily obtain from (6) and (8)

$$M(\mathbf{y}) \frac{\partial}{\partial \nu} \bar{\psi} = -\bar{p}, \quad M(\mathbf{y}) \frac{\partial}{\partial \nu} \bar{u} = T \frac{\partial}{\partial T} \bar{p} - \bar{p}, \quad M(\mathbf{y}) \frac{\partial}{\partial \nu} \bar{s} = \frac{\partial}{\partial T} \bar{p}. \quad (20)$$

We conclude that the volume derivatives of $\bar{\psi}(T, \nu, \mathbf{y})$, $\bar{u}(T, \nu, \mathbf{y})$ and $\bar{s}(T, \nu, \mathbf{y})$ are fully determined by the pressure $\bar{p}(T, \nu, \mathbf{y})$.

Definition of the specific heats. The specific enthalpy is defined by $M(\mathbf{y})\tilde{h}(T, p, \mathbf{y}) = M(\mathbf{y})\tilde{u}(T, p, \mathbf{y}) + p \cdot \tilde{\nu}(T, p, \mathbf{y})$. The derivatives of specific internal energy and the specific enthalpy with respect to temperature T represent the specific heat at constant volume and the specific heat at constant pressure, respectively, i.e.

$$c_v(T, \nu, \mathbf{y}) := \frac{\partial \tilde{u}(T, \nu, \mathbf{y})}{\partial T}, \quad c_p(T, p, \mathbf{y}) := \frac{\partial \tilde{h}(T, p, \mathbf{y})}{\partial T}. \quad (21)$$

While c_p can often be measured easily in experiments, in many cases c_v is more easy to treat in the constitutive theory. According to [BDD23] the important difference of the specific heats satisfies

$$c_p - c_v = \frac{T}{M(\mathbf{y})} \frac{\partial \tilde{\nu}}{\partial T} \frac{\partial \bar{p}}{\partial T} \geq 0. \quad (22)$$

If in particular the pressure is a linear function of temperature, then we conclude from (20) that $\frac{\partial}{\partial \nu} c_v(T, \nu, \mathbf{y}) = 0$. Using (6), we infer from the definition (21) that the specific entropy $\bar{s}(T, \nu, x) := \hat{s}(T, \nu^{-1} \mathbf{y})$ satisfies

$$\frac{\partial}{\partial T} \bar{s} = \frac{c_v}{T}. \quad (23)$$

Representations of specific internal energy and specific entropy.

Integrating (20) and (21) with respect to ν and T , respectively, we deduce a representation for the specific internal energy,

$$\begin{aligned} M(\mathbf{y})\bar{u}(T, \nu, \mathbf{y}) &= M(\mathbf{y})\bar{u}(T^{\text{ref}}, \nu^{\text{ref}}, \mathbf{y}) + M(\mathbf{y}) \int_{T^{\text{ref}}}^T c_v(\theta, \nu^{\text{ref}}, \mathbf{y}) d\theta \\ &\quad + \int_{\nu^{\text{ref}}}^{\nu} (T \frac{\partial}{\partial T} \bar{p} - \bar{p})(T, \xi, \mathbf{y}) d\xi. \end{aligned} \quad (24)$$

Integrating the specific heat at constant volume and the thermal equation of state with respect to T and ν , respectively, we derive for specific entropy the representation

$$\begin{aligned} M(\mathbf{y})\bar{s}(T, \nu, \mathbf{y}) &= M(\mathbf{y})\bar{s}(T^{\text{ref}}, \nu^{\text{ref}}, \mathbf{y}) + M(\mathbf{y}) \int_{T^{\text{ref}}}^T \frac{c_v}{\theta}(\theta, \nu^{\text{ref}}, \mathbf{y}) d\theta \\ &\quad + \int_{\nu^{\text{ref}}}^{\nu} \frac{\partial}{\partial T} \bar{p}(T, \xi, \mathbf{y}) d\xi. \end{aligned} \quad (25)$$

The specific free energy may be calculated from (24) and (25) as $\bar{\psi}(T, \nu, \mathbf{y}) = \bar{u}(T, \nu, \mathbf{y}) - T\bar{s}(T, \nu, \mathbf{y})$. Thus a constitutive model can be based on assumptions on the functions $\bar{p}(T, \nu, \mathbf{y})$, $c_v(T, \nu^{\text{ref}}, \mathbf{y})$, $\bar{u}(T^{\text{ref}}, \nu^{\text{ref}}, \mathbf{y})$ and $\bar{s}(T^{\text{ref}}, \nu^{\text{ref}}, \mathbf{y})$.

3.3 The simple mixture model

For the simple mixture model, we make the following assumptions similar to [BDD23]:

Thermal equation of state. To describe changes of the molar volume due to thermal expansion, elastic compression and changes of the composition, we assume the following simple constitutive law for the pressure

$$\bar{p}^{\text{sim}}(T, \nu, \mathbf{y}) = p^{\text{ref}} + K \cdot \left(\frac{\nu^{\text{sim}}(T, \mathbf{y})}{\nu} - 1 \right), \quad (26a)$$

$$\nu^{\text{sim}}(T, \mathbf{y}) = \sum_{\alpha \in \mathcal{I}} v_{\alpha}^{\text{ref}} \beta_{\alpha}(T) \cdot y_{\alpha}. \quad (26b)$$

Here, $K > 0$ denotes the isotropic compression modulus, and v_{α}^{ref} for $\alpha \in \mathcal{I}$ are the molar volumes in a reference state with $T = T^{\text{ref}}$ and $p^{\text{sim}} = p^{\text{ref}}$. The functions $\beta_{\alpha}(T)$ describing the thermal expansion of constituent $\alpha \in \mathcal{I}$ have to satisfy $\beta_{\alpha}(T^{\text{ref}}) = 1$. In the vicinity of the reference temperature, a linearization may be applied as

$$\beta_{\alpha}(T) \approx 1 + \left(\frac{T}{T^{\text{ref}}} - 1 \right) T^{\text{ref}} \beta_{\alpha}^{\text{ref}}. \quad (27)$$

Specific heat at constant volume $\nu = \nu^{\text{ref}} = \nu^{\text{sim}}(T^{\text{ref}}, \mathbf{y})$. We choose for $c_v(T, \nu^{\text{sim}}, \mathbf{y})$ a simple linear approach with respect to y_{α} , that does not depend on temperature, i.e.

$$M(\mathbf{y}) c_v(T, \nu^{\text{sim}}, \mathbf{y}) = \sum_{\alpha \in \mathcal{I}} m_{\alpha} c_{\alpha}^{\text{ref}} y_{\alpha}, \quad (28)$$

where the constant $c_{\alpha}^{\text{ref}} = c_{\alpha}^{\text{ref}}(\nu^{\text{sim}})$ are the specific heat constants of the pure constituents.¹ If in (26a) the pressure depends only linearly on temperature, then we conclude from (20) that $c_v(T, \nu, \mathbf{y})$ does not depend on the volume and c_{α}^{ref} is independent of ν^{sim} .

Specific entropy and specific internal energy at $T = T^{\text{ref}}$ and $\nu = \nu^{\text{ref}} = \nu^{\text{sim}}(T^{\text{ref}}, \mathbf{y})$. The essential ingredient of a simple mixture is a Boltzmann-typ logarithmic mixing contribution in addition to the purely linear approach, viz.

$$M(\mathbf{y}) \bar{u}(T^{\text{ref}}, \nu^{\text{sim}}, \mathbf{y}) = \sum_{\alpha \in \mathcal{I}} m_{\alpha} u_{\alpha}^{\text{ref}} y_{\alpha}, \quad (29a)$$

$$M(\mathbf{y}) \bar{s}(T^{\text{ref}}, \nu^{\text{sim}}, \mathbf{y}) = \sum_{\alpha \in \mathcal{I}} m_{\alpha} s_{\alpha}^{\text{ref}} y_{\alpha} - \sum_{\alpha \in \mathcal{I}} k_B \ln(y_{\alpha}) y_{\alpha}, \quad (29b)$$

where the constants $u_{\alpha}^{\text{ref}} = u_{\alpha}(T^{\text{ref}}, \nu^{\text{sim}})$ and $s_{\alpha}^{\text{ref}} = s_{\alpha}(T^{\text{ref}}, \nu^{\text{sim}})$, for $\alpha \in \mathcal{I}$, are the energy constants and the entropy constants for the pure constituents, respectively.²

¹ While for pure uncharged substances these constants may be found in tables, they will not be available for solvated ions.

²Same as in footnote 1 applies here.

Free energy density and chemical potentials of a simple mixture.

Application of the above the simple mixture assumptions (26)-(29) to the representations (24) and (25) with $\nu^{\text{ref}} = \nu^{\text{sim}}(T^{\text{ref}}, \mathbf{y})$ yields the free energy density. We rewrite the obtained result in terms of the variable $(T, (n_\alpha)_{\alpha \in \mathcal{I}})$ because this is the set of variables to calculate the chemical potentials. We have

$$\begin{aligned} \rho \hat{\psi}^{\text{sim}} = & \sum_{\alpha \in \mathcal{I}} n_\alpha m_\alpha \psi_\alpha^{\text{ref}} + \sum_{\alpha \in \mathcal{I}} n_\alpha m_\alpha c_\alpha^{\text{ref}} \cdot \left(T - T^{\text{ref}} - T \ln \left(\frac{T}{T^{\text{ref}}} \right) \right) \\ & + k_B T \sum_{\alpha \in \mathcal{I}} n_\alpha \ln \left(\frac{n_\alpha}{n} \right) - \sum_{\alpha \in \mathcal{I}} n_\alpha m_\alpha s_\alpha^{\text{ref}} \cdot (T - T^{\text{ref}}) \\ & + (K - p^{\text{ref}}) \left(1 - \sum_{\alpha \in \mathcal{I}} n_\alpha v_\alpha^{\text{ref}} \beta_\alpha(T) \right) + K \sum_{\alpha \in \mathcal{I}} n_\alpha v_\alpha^{\text{ref}} \beta_\alpha(T) \cdot \ln \left(\sum_{\alpha \in \mathcal{I}} n_\alpha v_\alpha^{\text{ref}} \beta_\alpha(T) \right) \end{aligned} \quad (30)$$

where we set the reference energies ψ_α^{ref}

$$\psi_\alpha^{\text{ref}} = u_\alpha^{\text{ref}} - T^{\text{ref}} s_\alpha^{\text{ref}}. \quad (31)$$

With the definition of the reference Gibbs energies $g_\alpha^{\text{ref}} = m_\alpha \psi_\alpha^{\text{ref}} + v_\alpha^{\text{ref}} p^{\text{ref}}$, the chemical potentials then are

$$\begin{aligned} \hat{\mu}_\alpha^{\text{sim}} = & g_\alpha^{\text{ref}} + p^{\text{ref}} v_\alpha^{\text{ref}} \cdot (\beta_\alpha(T) - 1) + m_\alpha c_\alpha^{\text{ref}} \cdot \left(T - T^{\text{ref}} - T \ln \left(\frac{T}{T^{\text{ref}}} \right) \right) \\ & + k_B T \ln \left(\frac{n_\alpha}{n} \right) - m_\alpha s_\alpha^{\text{ref}} \cdot (T - T^{\text{ref}}) \\ & + K v_\alpha^{\text{ref}} \beta_\alpha(T) \cdot \ln \left(\sum_{\gamma \in \mathcal{I}} n_\gamma v_\gamma^{\text{ref}} \beta_\alpha(T) \right). \end{aligned} \quad (32)$$

3.4 Electric field contribution of a single ion

We aim at characterizing the energetic difference caused by the fact that the electrolyte is not a neutral medium but rather a mixture of charged particles. Therefore, we consider a bulk electrolyte outside of boundary layers, such that it is locally electroneutral on the macroscopic scale. As the main material property of the electrolyte we only consider its dielectric susceptibility which on the macroscopic scale may depend on the local temperature and composition, i.e. the number densities n_γ . Then, we turn to a more microscopic scale, where we take the number densities n_γ from the more macroscopic scale to now define the far field $n_\gamma^\infty = n_\gamma$ and assume that the temperature T , the susceptibility χ and its temperature derivative $\frac{\partial}{\partial T} \chi$ are homogeneous in space, depending only on T and the far field number densities n_γ^∞ . We select an arbitrary solvated ion from any of the species $\gamma \in \mathcal{I}$ and further refer it by using the subscript $*$. For this selected ion carrying the total charge $z_* e_0$, we choose the reference frame such that this

ion is fixed at the origin. Except while undergoing the dissociation reaction, no other charged particles are allowed to enter into a sphere of radius $R_* > 0$ containing the selected bare center ion together with its solvation shell. The radius R_* may depend on the temperature. As it will turn out, it is not necessary to postulate any assumptions on the the spatial charge distribution inside of the solvated ion, i.e. for $r < R_*$.

The electric potential ϕ due to the single selected ion in an unbounded space is in general determined by the Poisson boundary value problem

$$-(1 + \chi)\varepsilon_0\Delta\phi = n^F \quad \text{for } r > 0 , \quad (33a)$$

$$\llbracket\phi\rbracket = 0 , \quad \llbracket(1 + \chi)\varepsilon_0\frac{\partial}{\partial r}\phi\rbracket = 0 \quad \text{at } r = R_* , \quad (33b)$$

$$\phi \rightarrow 0 \quad \text{for } r \rightarrow \infty , \quad (33c)$$

where n^F denotes the free charge density. In order to account for the character of electrolytes as mixture of a charged particles, we have to find the difference of the electric energy between i) ions in a electrically neutral medium, i.e. $n^F = 0$, and ii) ions in locally charged medium.

Ion in neutral medium. Assume first that the selected ion is surrounded by an electrically neutral medium with susceptibility χ , i.e. $n^F = 0$ for all $R_* < r$. Then, the net charge z_*e_0 inside the inner domain $r < R_*$ causes in the outer domain the electric potential

$$\phi_0(r) = \frac{z_*e_0}{4\pi\varepsilon_0} \frac{1}{1 + \chi} \frac{1}{r} \quad \text{for } R_* < r . \quad (34)$$

Ion in electrolyte. In a continuum description of electrolytes, a net charge z_*e_0 inside a sphere of radius R_* causes the formation of an oppositely charged electrolyte layer around this sphere. It is well known that electrolyte boundary layers at strongly charged surfaces may become highly concentrated and steric effects can not be neglected in order to limit charge accumulation in the layer. In the present problem however, the total charge of the whole boundary layer is necessarily limited to just the opposite charge of the single selected ion, which makes volume exclusion effects insignificant here. Thus, steric Poisson-Boltzmann models like e.g. [DGM13], will not do not offer a decisive advantage over the classical Poisson-Boltzmann approach.³ To derive an analytic expressions for the energy, we linearize the Poisson equation (33a) around the far field state. We note that before already the susceptibility χ and $\frac{\partial}{\partial T}\chi$ have been frozen to their far field values. For given reference temperature T^{ref} and reference number density n^{ref} , we introduced the Debye

³The negligibly impact of steric effects on the electric field around the selected ion is illustrated by numerical solution of the problem (33) in the supporting material.

screening length ℓ as a reference length and define Λ by

$$\ell = \sqrt{\frac{\varepsilon_0 k_B T^{\text{ref}}}{e_0^2 n^{\text{ref}}}} , \quad (\Lambda \ell)^2 = \frac{T^{\text{ref}}}{T} \frac{1}{1 + \chi} \sum_{\gamma \in \mathcal{I}} z_\gamma^2 \frac{n_\gamma^\infty}{n^{\text{ref}}} . \quad (35)$$

We remark that while ℓ depends on the chosen reference state, the inverse length Λ does not. Next, we approximate

$$n^{\text{F}} = e_0 \sum z_\gamma n_\gamma \exp\left(-z_\gamma \frac{e_0}{k_B T} \phi\right) \approx -(1 + \chi) \varepsilon_0 \Lambda^2 \phi \quad \text{for } R_* < r . \quad (36)$$

The solution of the linearized Poisson problem (33) and (36) is

$$\phi(r) = \frac{z_* e_0}{4\pi \varepsilon_0} \frac{1}{1 + \chi} \frac{1}{1 + \Lambda R_*} \frac{\exp(-\Lambda(r - R_*))}{r} \quad \text{for } R_* < r . \quad (37)$$

Interaction energy. Our basic assumption is that the general thermodynamic relations (5)-(6) from Sect. 2.1 are applicable on the scale of single ion problem. Thus, the densities of internal energy and entropy are $(\hat{\chi} + T \frac{\partial}{\partial T} \hat{\chi}) \frac{\varepsilon_0}{2} |\nabla \phi|^2$ and $\frac{\partial}{\partial T} \hat{\chi} \frac{\varepsilon_0}{2} |\nabla \phi|^2$, respectively. Internal energy and entropy are additive quantities, such that the r -dependence of the electric field may simply be smoothed out by taking the volume integral over both densities. Finally, we define internal energy and entropy due to ion-ion interaction as the difference between the two above scenarios. Hence, the interaction of an individual ion with its surrounding leads to the following contributions to energy and entropy

$$U_*^W = \frac{\varepsilon_0}{2} \int_{\mathbb{R}^3} (\chi + T \frac{\partial}{\partial T} \chi) (|\nabla \phi|^2 - |\nabla \phi_0|^2) dx , \quad (38a)$$

$$S_*^W = \frac{\varepsilon_0}{2} \int_{\mathbb{R}^3} \frac{\partial}{\partial T} \chi (|\nabla \phi|^2 - |\nabla \phi_0|^2) dx . \quad (38b)$$

By means of partial integration this can be reformulated in the way

$$U_*^W = \underbrace{2\pi \int_{r < R_*} \frac{\chi + T \frac{\partial}{\partial T} \chi}{1 + \chi} (\phi - \phi_0) n^{\text{F}} r^2 dr}_{=U_*^{W'}} + \underbrace{2\pi \int_{r > R_*} \frac{\chi + T \frac{\partial}{\partial T} \chi}{1 + \chi} \phi n^{\text{F}} r^2 dr}_{=U_*^{W''}} \quad (39)$$

By straightforward calculation, cf. the supplementary material, we get

$$U_*^{W'} = -z_*^2 \frac{e_0^2}{8\pi \varepsilon_0} \frac{\chi + T \frac{\partial}{\partial T} \chi}{(1 + \chi)^2} \Lambda \frac{1}{1 + \Lambda R_*} , \quad (40a)$$

$$U_*^{W''} = -z_*^2 \frac{e_0^2}{8\pi \varepsilon_0} \frac{\chi + T \frac{\partial}{\partial T} \chi}{(1 + \chi)^2} \frac{\Lambda}{2} \frac{1}{(1 + \Lambda R_*)^2} . \quad (40b)$$

We define for abbreviation

$$a := \frac{e_0^2}{8\pi\epsilon_0} \frac{n^{\text{ref}}}{\ell} , \quad F_*(R_*, \Lambda\ell) := \Lambda\ell \frac{3 + 2\Lambda R_*}{(1 + \Lambda R_*)^2} . \quad (41)$$

In total, we get from the interaction of the selected ion with its surrounding the contributions to internal energy and entropy

$$U_*^W = -\frac{a}{2} \frac{z_*^2}{n^{\text{ref}}} \frac{\chi + T \frac{\partial}{\partial T} \chi}{(1 + \chi)^2} F_*(R_*, \Lambda\ell) , \quad (42a)$$

$$S_*^W = -\frac{a}{2} \frac{z_*^2}{n^{\text{ref}}} \frac{\frac{\partial}{\partial T} \chi}{(1 + \chi)^2} F_*(R_*, \Lambda\ell) . \quad (42b)$$

3.5 Free energy contribution due to electric interaction

The above construction can be repeated for every ion in the mixture. In the volume V occupied by the electrolyte, let there be $N_\gamma/V = n_\gamma$ ions of species $\gamma \in \mathcal{I}$ and set $n_\gamma^\infty = n_\gamma$. Recalling (35), we introduce the dimensionless quantities

$$\tau = \frac{T}{T^{\text{ref}}} , \quad \lambda = \Lambda\ell = \sqrt{\frac{1}{(1 + \chi) \tau} \sum_{\gamma \in \mathcal{I}} z_\gamma^2 \frac{n_\gamma}{n^{\text{ref}}}} . \quad (43)$$

and take (41) with $R_\gamma = R_\gamma(\tau)$ and $\lambda = \lambda(\tau, (n_\gamma)_\gamma)$ to define for $\gamma \in \mathcal{I}$

$$F_*(R_\gamma, \lambda) = \lambda \frac{3 + 2\lambda R_\gamma/\ell}{(1 + \lambda R_\gamma/\ell)^2} . \quad (44)$$

To obtain internal energy and entropy due to the electrical interaction between the ions, we must sum up the contributions of all constituents $\gamma \in \mathcal{I}$, viz.

$$U^D = \sum N_\gamma U_\gamma^W , \quad S^D = \sum N_\gamma S_\gamma^W , \quad (45)$$

where U_γ^W and S_γ^W are given by (42). Dividing by the volume of the electrolyte mixture and setting $U^W/V = \rho \hat{u}^D$, $S^W/V = \rho \hat{s}^D$ yields contributions to the densities of internal energy and entropy, viz.

$$\rho \hat{u}^D = -\frac{a}{2} \frac{\chi + T \frac{\partial}{\partial T} \chi}{(1 + \chi)^2} \sum_{\gamma \in \mathcal{I}} z_\gamma^2 \frac{n_\gamma}{n^{\text{ref}}} F_*(R_\gamma, \lambda) , \quad (46a)$$

$$\rho \hat{s}^D = -\frac{a}{2} \frac{\frac{\partial}{\partial T} \chi}{(1 + \chi)^2} \sum_{\gamma \in \mathcal{I}} z_\gamma^2 \frac{n_\gamma}{n^{\text{ref}}} F_*(R_\gamma, \lambda) . \quad (46b)$$

Finally, applying $\rho \hat{\psi}^D = \rho \hat{u}^D - T \rho \hat{s}^D$, the resulting free energy density is

$$\rho \hat{\psi}^D = -\frac{a}{2} \frac{\chi}{(1 + \chi)^2} \sum_{\gamma \in \mathcal{I}} z_\gamma^2 \frac{n_\gamma}{n^{\text{ref}}} F(R_\gamma, \lambda) \quad \text{with} \quad F(R_\gamma, \lambda) = F_*(R_\gamma, \lambda) . \quad (47)$$

The main reason to distinguish $F(R_\gamma, \lambda)$ from $F_*(R_\gamma, \lambda)$ is for later comparison with the standard derivation procedure of a Debye-Hückel energy in the way of [DH23a].

Temperature dependence of the susceptibility. We note that unlike the simple mixture model above, neither the internal energy density $\rho \hat{u}^D$ nor the entropy density $\rho \hat{s}^D$ in (46) are calculated by means of general representations like (24) and (25). Thus, in order to guarantee thermodynamic consistency, the constitutive functions (46) and (47) need to satisfy the thermodynamic conditions (6) which must now be exploited for vanishing macroscopic electric field $\mathbf{E} \approx 0$. Due to the above construction (47) for $\rho \hat{\psi}^D$, the validity of (6a) directly implies (6b). Thus it remains to check (6a). Applying (46b) and (47) to $\rho \hat{s}^D = -\frac{\partial}{\partial T} \rho \hat{\psi}^D$, we get

$$\frac{\partial}{\partial T} \left(\frac{1}{1+\chi} \right) \sum_{\gamma \in \mathcal{I}} z_\gamma^2 \frac{n_\gamma}{n^{\text{ref}}} F(R_\gamma, \lambda) = \frac{\partial}{\partial T} \left(\left(\frac{1}{1+\chi} - \frac{1}{(1+\chi)^2} \right) \sum_{\gamma \in \mathcal{I}} z_\gamma^2 \frac{n_\gamma}{n^{\text{ref}}} F(R_\gamma, \lambda) \right), \quad (48)$$

what we can rearrange as

$$0 = 2 \frac{1+\chi}{\chi} \frac{\frac{\partial}{\partial T} \chi}{(1+\chi)^2} \sum_{\gamma \in \mathcal{I}} z_\gamma^2 \frac{n_\gamma}{n^{\text{ref}}} F(R_\gamma, \lambda) + \frac{\partial}{\partial T} \left(\sum_{\gamma \in \mathcal{I}} z_\gamma^2 \frac{n_\gamma}{n^{\text{ref}}} F(R_\gamma, \lambda) \right). \quad (49)$$

Using the identity $\frac{\frac{\partial}{\partial T} \chi}{(1+\chi)\chi} = \frac{\partial}{\partial T} \ln \left(\frac{\chi}{1+\chi} \right)$, we infer

$$0 = \frac{\partial}{\partial T} \ln \left(\left(\frac{\chi}{1+\chi} \right)^2 \sum_{\gamma \in \mathcal{I}} z_\gamma^2 \frac{n_\gamma}{n^{\text{ref}}} F(R_\gamma, \lambda) \right). \quad (50)$$

We conclude that the argument of the logarithm has to be independent of temperature. Consequently, the temperature dependence of the susceptibility function $\chi(T, (n_\alpha)_\alpha)$ is determined by the temperature dependence of the inverse length $\lambda(T, (n_\alpha)_\alpha)$.

Contributions to chemical potentials and pressure. We abbreviate

$$\mathcal{L}_\chi = \sum_{\alpha \in \mathcal{I}} n_\alpha \frac{\partial}{\partial n_\alpha} \chi, \quad D = 1 + \chi, \quad (51)$$

$$\mathcal{F} = \sum_{\gamma \in \mathcal{I}} z_\gamma^2 \frac{n_\gamma}{n^{\text{ref}}} F(R_\gamma, \lambda), \quad d\mathcal{F} = \sum_{\gamma \in \mathcal{I}} z_\gamma^2 \frac{n_\gamma}{n^{\text{ref}}} \frac{\partial}{\partial \lambda} F(R_\gamma, \lambda). \quad (52)$$

We note that whenever the above operator \mathcal{L} acts on a homogeneous function h of degree one with respect to the number densities, then $\mathcal{L}h = h$. We check the identities

$$\frac{\partial}{\partial \chi} \frac{\chi}{D^2} = \frac{1 - \chi}{D^3}, \quad \frac{\partial}{\partial n_\alpha} \lambda = \frac{1}{2} \left(\frac{1}{\tau D \lambda} \frac{z_\alpha^2}{n^{\text{ref}}} - \frac{\lambda}{D} \frac{\partial}{\partial n_\alpha} \chi \right). \quad (53a)$$

Then, the contributions to the free energy the chemical potentials and pressure, respectively, are

$$\rho \hat{\psi}^{\text{D}} = -\frac{a}{2} \frac{\chi}{D^2} \mathcal{F}, \quad (54a)$$

$$\hat{\mu}_\alpha^{\text{D}} = -\frac{a}{2} \frac{\chi}{D^2} \left[\frac{z_\alpha^2}{n^{\text{ref}}} \left(F(R_\alpha, \lambda) + \frac{1}{\tau D \lambda^2} \frac{\lambda}{2} d\mathcal{F} \right) - \left(\frac{\chi - 1}{\chi} \mathcal{F} + \frac{\lambda}{2} d\mathcal{F} \right) \frac{\frac{\partial}{\partial n_\alpha} \chi}{D} \right], \quad (54b)$$

$$\hat{p}^{\text{D}} = -\frac{a}{2} \frac{\chi}{D^2} \left(\frac{\lambda}{2} d\mathcal{F} - \left(\frac{\chi - 1}{\chi} \mathcal{F} + \frac{\lambda}{2} d\mathcal{F} \right) \frac{\mathcal{L}\chi}{D} \right). \quad (54c)$$

3.6 Summary and a first assessment of the material model

Within boundary layers, we propose a constitutive model based on the simple mixture model and an explicit energy contribution due to the electric field, viz.

$$\text{(BL)} \begin{cases} \rho \psi = \rho \psi^{\text{sim}}(T, (n_\alpha)_{\alpha \in \mathcal{I}}) - \chi \frac{\varepsilon_0}{2} |\mathbf{E}|^2, \\ \mu_\alpha = \mu_\alpha^{\text{sim}}(T, (n_\alpha)_{\alpha \in \mathcal{I}}) - \frac{\partial}{\partial n_\alpha} \chi \frac{\varepsilon_0}{2} |\mathbf{E}|^2, \\ p = p^{\text{sim}} = p^{\text{ref}} + K \cdot \left(\sum_{\alpha \in \mathcal{I}} v_\alpha^{\text{ref}} \beta_\alpha(T) n_\alpha - 1 \right), \end{cases} \quad (55)$$

with $\rho \psi^{\text{sim}}$ according to (30). To this model, a (quasi-)incompressible limit was applied in [DGM13, LGD16, DGM18, LM22] and analyzed in detail in [BDD23]. For $p^{\text{ref}} \ll K$ a constraint $\sum_{\alpha \in \mathcal{I}} v_\alpha^{\text{ref}} \beta_\alpha(T) n_\alpha = 1$ arises, requiring p to take the role of an independent variable.

In homogeneous bulk domains, where on the macroscopic scale the electric field vanishes, i.e. $\mathbf{E} \approx 0$, we propose

$$\text{(HB)} \begin{cases} \rho \psi = \rho \psi^{\text{sim}}(T, (n_\alpha)_{\alpha \in \mathcal{I}}) + \rho \psi^{\text{D}}(T, (n_\alpha)_{\alpha \in \mathcal{I}}), \\ \mu_\alpha = \mu_\alpha^{\text{sim}}(T, (n_\alpha)_{\alpha \in \mathcal{I}}) + \mu_\alpha^{\text{D}}(T, (n_\alpha)_{\alpha \in \mathcal{I}}), \\ p = p^{\text{ref}} + K \cdot \left(\sum_{\alpha \in \mathcal{I}} v_\alpha^{\text{ref}} \beta_\alpha(T) n_\alpha - 1 \right) + p^{\text{D}}(T, (n_\alpha)_{\alpha \in \mathcal{I}}), \end{cases} \quad (56)$$

with $\rho \psi^{\text{sim}}$ according to (30) and $\rho \psi^{\text{D}}$ according to (47). Since both contributions p^{sim} and p^{D} in general need to balance each other, the consideration of a (quasi-)incompressible limit is not suitable in this context.

We choose as reference values room temperature a number density n^{ref} corresponding to a solution of 1 mol L^{-1} . This implies for the Debye screening length

$$T^{\text{ref}} = 298.15 \text{ K} , \quad n^{\text{ref}} = 1000 \mathcal{N}_A \quad \Longrightarrow \quad \ell \approx 0.04856 \text{ nm} . \quad (57)$$

With the specific volume of water at $T = T^{\text{ref}}$ we conclude

$$v_S^{\text{ref}} = (55.345 n^{\text{ref}})^{-1} \quad \Longrightarrow \quad R_S(T^{\text{ref}}) = \sqrt[3]{\frac{3}{4\pi}} v_S^{\text{ref}} \approx 0.1928 \text{ nm} \approx 4\ell . \quad (58)$$

Pressure contribution at $\tau = 1$. Let the total pressure p in the electrolyte be fixed at the outer reference pressure, i.e. $p \stackrel{!}{=} p^{\text{ref}}$. For the elastic bulk modulus of water $K \approx 2.2 \times 10^{+9} \text{ J m}^{-3}$, we have with the above reference values $a/K \approx 0.65$. If we assume $\mathcal{L}_\chi/\chi \approx 1$, $\chi - 1 \approx D$ and $D - \mathcal{L}_\chi \ll D$, we can deduce from (54c) and (56) the approximate relation

$$\frac{p^{\text{D}}}{K} = -\frac{a}{2K} \frac{\chi}{D^2} \left(\frac{\lambda}{2} d\mathcal{F} \frac{D - \mathcal{L}_\chi}{D} - \frac{\chi - 1}{D} \mathcal{F} \frac{\mathcal{L}_\chi}{\chi} \right) \approx \frac{1}{D} \frac{a}{2K} \mathcal{F} . \quad (59)$$

For $\lambda < 0.15$, the function F is in less than, or in the order of 0.1, depending on R_α . Assuming $\mathcal{F} = \tau D \lambda^2 F(R_\alpha, \lambda)$, for any $\alpha \in \mathcal{I}$, we can conclude that $p^{\text{D}}/K \approx \frac{\lambda^2}{2} \frac{a}{K} F(R_\alpha, \lambda) \approx 0.001$ for $\lambda < 0.15$. Thus, we can expect the pressure contribution p^{D} to be smaller than the bulk modulus of water K by a factor in the order of 1000. This coincides with the estimate of Debye-Hückel [DH23a, before eq. (7)]. Accordingly, the absolute change of volume due to p^{D} can be expected small compared to elastic deformations. Neglecting this pressure contribution, we conclude from (56)

$$\underline{\tau = 1, p = p^{\text{ref}}, p^{\text{D}} \ll K:} \quad \sum_{\alpha \in \mathcal{I}} v_\alpha^{\text{ref}} n_\alpha = 1 - \frac{p^{\text{D}}}{K} \approx 1 . \quad (60)$$

In the following Sect. 4 however, it turns out that for the apparent molar volume of the solution, the pressure contribution p^{D} can not be neglected.

Temperature dependence of susceptibility. To study the implications of the thermodynamic compatibility condition (50) on the temperature dependence of the susceptibility, we choose the most simple configuration of a symmetric $-1 : 1$ -electrolyte. For concentration less than 1 mol L^{-1} , we assume complete dissociation of the salt. Thus, we consider a mixture consisting only of the neutral solvent and solvated anions and cations, i.e. $\mathcal{I} = \{A, C, S\}$ with $-z_A = z_C = 1$ and $z_S = 0$. We let

$$\underline{\text{for complete dissociation}} \quad c = \frac{1}{2} \frac{n_A + n_C}{1000 \mathcal{N}_A} \quad (61)$$

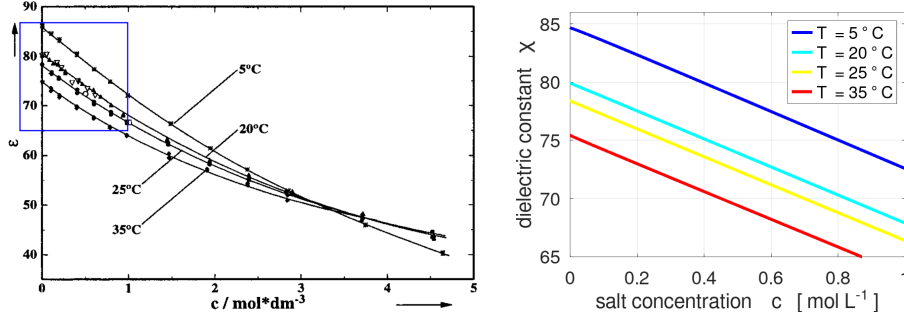


Figure 1: Left: Susceptibility $\chi(T, c)$ of aqueous NaCl solution, Figure from [BHM99, Fig. 1] reproduced with permission. Inside the marked box, the dielectric decrement is close to linear for salt concentration less than 1 mol L^{-1} . Right: computed susceptibility based on (64), where χ linear at $\tau = 1$ with $d = 12 \text{ L mol}^{-1}$ and $R_A = R_C = 8\ell$.

denote the electrolyte concentration in mol L^{-1} . Since equilibrium in an electrolyte bulk domain implies local electro-neutrality, cf. e.g. [DGM18], we can conclude $n_A = n_C = cn^{\text{ref}}$. For dilute solutions, there is often a decrease of the susceptibility with the electrolyte concentration observed, cf. [HRC48, BHM99]. Thus, we have a linear relation

$$\text{at } \tau = 1: \quad \chi = \chi_S^{\text{ref}} - d_A \frac{n_A}{1000\mathcal{N}_A} - d_C \frac{n_C}{1000\mathcal{N}_A} = \chi_S^{\text{ref}} - d \cdot c, \quad (62)$$

where $d = d_A + d_C$ is called the *dielectric decrement*. Assuming $p^D \ll K$, we use (60) to rewrite the susceptibility as a homogeneous function of the number densities, viz.

$$\text{at } \tau = 1: \quad \chi = \sum_{\alpha \in \mathcal{I}} \chi_\alpha^{\text{ref}} v_\alpha^{\text{ref}} n_\alpha, \quad (63a)$$

$$\text{with } \chi_\alpha^{\text{ref}} = \chi_S^{\text{ref}} - \frac{d_\alpha}{v_\alpha^{\text{ref}} n^{\text{ref}}} \quad \text{for } \alpha \in \{A, C\}. \quad (63b)$$

We abbreviate $D_1 = 1 + \chi(\tau = 1, (n_\alpha)_\alpha)$ and $\lambda_1 = \lambda(\tau = 1, (n_\alpha)_\alpha)$. The compatibility condition (50) then implies that D for any τ and c is determined by

$$\left(\frac{D-1}{D}\right)^2 \sum_{\gamma \in \mathcal{I}} z_\gamma^2 \frac{n_\gamma}{n^{\text{ref}}} F(R_\gamma(\tau), \lambda) = \left(\frac{D_1-1}{D_1}\right)^2 \sum_{\gamma \in \mathcal{I}} z_\gamma^2 \frac{n_\gamma}{n^{\text{ref}}} F(R_\gamma(1), \lambda_1). \quad (64)$$

For given τ and c , we set $n_S, D_1 = 1 + \chi(1, c, c, n_S)$ and $\lambda_1 = \lambda(1, c, c, n_S)$

according to

$$0 = \left(v_A^{\text{ref}} \beta_A(\tau) + v_C^{\text{ref}} \beta_C(\tau) \right) c + v_S^{\text{ref}} \beta_S(\tau) n_S - 1, \quad (65a)$$

$$0 = D_1 - 1 - \chi_S^{\text{ref}} v_S^{\text{ref}} n_S - \sum_{\alpha \in \{A, C\}} \chi_\alpha^{\text{ref}} v_\alpha^{\text{ref}} c \cdot n^{\text{ref}}, \quad (65b)$$

$$0 = \lambda_1^2 D_1 - 2c. \quad (65c)$$

Then, we determine $\lambda = \lambda(\tau, c, c, n_S)$ and $D(\tau, c, c, n_S)$ by solving the system

$$0 = \lambda^2 \tau D - 2c, \quad (65d)$$

$$0 = \sum_{\gamma \in \{A, C\}} \left[\sqrt{\frac{D_1}{\tau D}} \left(\frac{D-1}{D} \right)^2 \frac{F(R_\gamma, \lambda)}{\lambda} - \left(\frac{D_1-1}{D_1} \right)^2 \frac{F(R_\gamma(1), \lambda_1)}{\lambda_1} \right]. \quad (65e)$$

Fig. 1 shows the resulting $\chi(\tau, c)$ at four different temperatures, where the thermal expansion $\beta_S(\tau)$ in (65a) was taken according to the data fit [AM99, eq. (5)] for the values of expansion coefficient of pure water measured there. Literature values of d at $T^{\text{ref}} = 25^\circ \text{C}$ for many electrolyte solutions are discussed in [Mar13] and it is concluded that the accuracy of the given values in the literature is rather low, i.e. uncertainty is in the order of 1. We chose $d = 12$ for a NaCl solutions, compatible with [BHM99, Mar13]. We observe that for any $\tau \neq 1$ the computed susceptibility remains visually indistinguishable from straight lines. This result gives some justification to choose a homogeneous function $\chi(\tau = 1, c)$ regardless of whether the reference temperature T^{ref} was chosen more or less arbitrarily.

Although (50) and (64) can not directly be used to determine the thermal variation of the susceptibility $\chi_S(\tau)$ of the pure solvent, we can safely take the limit for $c \rightarrow 0$ in (65e). We infer

$$\frac{\chi_S(\tau)^2}{(\chi_S(\tau) + 1)^{5/2}} = \sqrt{\tau} \frac{(D_1 - 1)^2}{D_1^{3/2}} \quad \text{with} \quad D_1 = 1 + \frac{\chi_S^{\text{ref}}}{v_S^{\text{ref}} \cdot \beta_S(\tau)}, \quad (66)$$

and conclude that the thermodynamic compatibility condition (50) does not induce any dependence of the solvent susceptibility χ_S on the dissolved salt. However, (50) implies that the temperature dependence of χ_S is already fully encoded in the thermal expansion of the pure solvent.

Comparison to standard Debye-Hückel model. The density ρu^D of internal energy is one essential cornerstone of the original Debye-Hückel model [DH23a], as well as of the proposed model here. In both cases, it can be written in the form (46a), where here the quantity $f_\alpha(R_\alpha, \Lambda \ell)$ defined by (44) may also be rewritten as

$$F_*(R_\alpha, \Lambda \ell) = \Lambda \ell \frac{3 + 2\Lambda R_\alpha}{(1 + \Lambda R_\alpha)^2} = \frac{2\Lambda \ell}{1 + \Lambda R_\alpha} + \frac{\Lambda \ell}{(1 + \Lambda R_\alpha)^2}. \quad (67)$$

While the first term on the right hand side also occurs in [DH23a], the second term is missing there. The absence of the second term might be related to the conception of the selected ion as a point charge and following evaluation of the electric potential only in the origin.

In order to derive from ρu^D the free energy density $\rho\psi^D$, there are two common methods in the literature. The first method was proposed in [DH23a]. It assumes that the susceptibility is independent of temperature, i.e. $\frac{\partial}{\partial T}\chi = 0$, such that the formula (6b) for $\mathbf{E} = 0$ can be integrated with respect to temperature. This leads to a free energy density of the same structure as in (47), but instead of $F_\alpha(\Lambda\ell) = f_\alpha(\Lambda\ell)$ one gets

$$F(R_\alpha, \Lambda\ell) = -T \int \frac{F_*(R_\alpha, \Lambda\ell)}{T^2} dT . \quad (68)$$

Soon after the first derivation, the importance of a temperature dependent susceptibility was noticed, an alternative derivation was introduced [Deb24] based on a hypothetical reversible charging process at constant temperature. Both approaches yield the same result and they are therefore both generally accepted in the literature, although some weakness of their justification is usually mentioned.

Instead of *a-priori* assuming $\frac{\partial}{\partial T}\chi = 0$, we already incorporate the temperature dependence of the susceptibility in the inner energy density ρu^D and the density of entropy ρs^D , based on the general thermodynamic framework of Sect. 2.1 providing (6). Then, we can rely on both densities to directly derive the free energy density by the definition $\rho\psi^D = \rho u^D - T\rho s^D$, and thereby get *a-posteriori* the thermodynamic compatibility condition (50) restricting the generality of $\frac{\partial}{\partial T}\chi(T, (n_\alpha)_\alpha)$.

4 Application to bulk domains of binary electrolytes

4.1 Description of electrolytes

We consider an electrolyte that is prepared by dissolving some neutral salt E in a neutral solvent S. The salt dissociates into negatively charged anions and positively charged cations. Many solvents, in particular water, have a molecular structure that consists of microscopic dipoles. These dipoles cause a microscopic electrostatic interaction between charged ions and solvent molecules. This interaction, which is known as solvation, leads to the formation of larger complexes by clustering of solvent molecules around a center ion. The solvation has a profound impact on the mixing entropy within the electrolyte model [LGD16] because solvent molecules that are bounded by a center ion do not participate in the entropic interaction with the other constituents of the electrolytic mixture. Therefore, we choose the solvated ions as the constituents of the mixture and refer to the solvated anions and cations as A and C, respectively. Neglecting any other species,

Table 2: Reference values and material parameters for an aqueous NaCl electrolyte.

$T^{\text{ref}} = 25^\circ\text{C}$	$n^{\text{ref}} = 1000\mathcal{N}_A$
$m_S = 18.0152833 \text{ g mol}^{-1}$	$z_S = 0$
$v_S^{\text{ref}} = (55.345 n^{\text{ref}})^{-1}$	$K = 2.2 \times 10^{+9} \text{ J m}^{-3}$
$\chi_S^{\text{ref}} = 78.38$	
$m_E = 58.443 \text{ g mol}^{-1}$	$z_E = 0$
$z_A = -z_C = 1$	
$d = 12 \text{ L mol}^{-1}$	

the index set of the electrolyte is then given as $\mathcal{I} = \{\text{A, C, E, S}\}$. We use material parameters to represent an aqueous solution of NaCl according to Table 2.

Input ratio of the mixture. At any time after the initial state, the actual total volume occupied by the electrolytic mixture is denoted by V . By N_α and $M_\alpha = m_\alpha N_\alpha$, we denote the total number of molecules and the total mass of species $\alpha \in \mathcal{I}$ inside the volume V , respectively. The electrolytic solution is prepared from initially N_S^0 solvent molecules, occupying at the temperature T the initial volume

$$V_S = V_S^{\text{ref}} \beta_S(T), \quad V_S^{\text{ref}} = v_S^{\text{ref}} N_S^0, \quad (69)$$

with the thermal volume expansion function $\beta_S(T)$ and the specific volume v_S^{ref} of the solvent at the reference temperature T^{ref} as introduced in Sect. 3.3. Then, N_E^0 molecules of the electrically neutral salt are added. To characterize the electrolyte mixture, we introduce the dimensionless *total input ratio* σ and the *molality* m in mol kg^{-1} as

$$\sigma = \frac{N_E^0}{N_S^0}, \quad m = \frac{1}{\mathcal{N}_A} \frac{N_E^0}{M_S^0} = \frac{1}{m_S \mathcal{N}_A} \sigma, \quad (70)$$

respectively. A molality $m = 1 \text{ mol kg}^{-1}$ of a salt E in water corresponds to the input ratio $\sigma \approx 0.018$. Alternatively, it is possible to prepare a mixture with a specified *molar concentration* c in mol L^{-1} , with

$$c = \frac{N_E^0}{1000\mathcal{N}_A V}, \quad (71)$$

by taking N_E^0 molecules of the salt and adding as much solvent as needed until the mixture reaches the actual volume V . In this case, the number N_S^0 of solvent molecules is a-priori unknown.

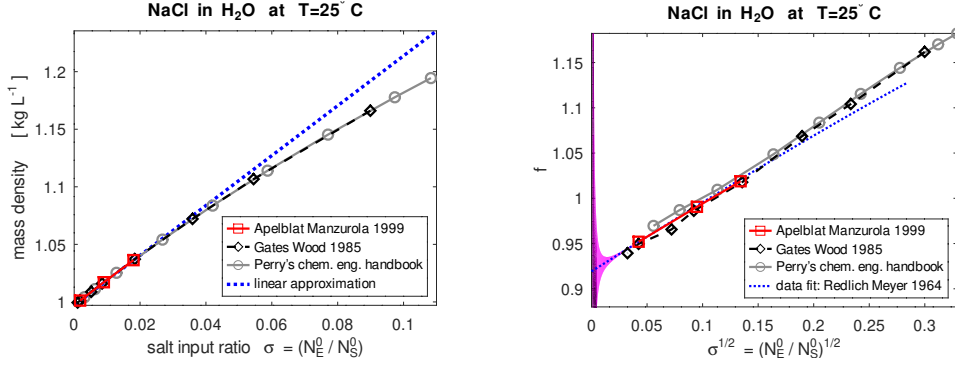


Figure 2: Left: Mass density of aqueous NaCl solution at 25° C over salt concentration. from measured density ρ of [CCM80, AW81, GW85, AM99, PG08]. Right: Volume change factor f over salt input σ calculated by (74) from measured density ρ and data fit of [RM64].

Volume and mass density. To relate in a homogeneous system the actual volume V of the mixture to the initial volume V_S of the pure solvent, we introduce dimensionless *volume factor* f , and equivalently the *apparent molar volume* $\Phi_V = 1000\mathcal{N}_A v_S^{\text{ref}} \beta_S(T) \cdot 1000f$, with the dimensions L mol^{-1} , cf. e.g, [RM64, Mil71], such that

$$V = V_S^{\text{ref}} \beta_S(T) \cdot (1 + f \sigma) , \quad (72a)$$

$$= V_S + \frac{1}{1000} \Phi_V \frac{N_E^0}{1000\mathcal{N}_A} . \quad (72b)$$

The mass density and the molar concentration of the homogeneous mixture are

$$\rho = \frac{M_S^0 + M_E^0}{V} = \frac{1}{v_S^{\text{ref}} \beta_S(T)} \frac{m_S + m_E \sigma}{1 + f \sigma} , \quad (73a)$$

$$c = \frac{1}{v_S^{\text{ref}} \beta_S(T)} \frac{\sigma}{1 + f \sigma} \frac{1}{1000\mathcal{N}_A} . \quad (73b)$$

Conversely, we can also express the volume factor f in dependence of ρ as

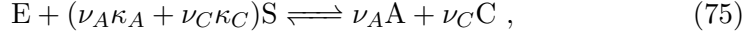
$$f = \frac{m_E}{v_S^{\text{ref}} \beta_S(T)} \frac{1}{\rho} + \left(\frac{m_S}{v_S^{\text{ref}} \beta_S(T)} \frac{1}{\rho} - 1 \right) \frac{1}{\sigma} . \quad (74)$$

Thus, taking data from density measurements, it is possible to calculate f as a function of σ without applying any model assumption at all. In Fig. 2, we see that the mass density of the solution can already be approximated by a linear relation to the salt input, at least for concentrations below 2 mol L^{-1} . The deviation from the linear behavior is caused by variations of the volume factor f . Experimental data shows in Fig. 2 a close to linear behavior of f

when plotted as a function of $\sqrt{\sigma}$. The values for the linear approximation are taken from [RM64]). The data of [PG08] show a positive offset against the linear data fit of $f(\sqrt{\sigma})$ in [RM64]). For dilute solutions, the data of [CCM80, AW81, GW85, AM99] agrees well with the linear fit. Then around salt molality in the range of 1 mol kg^{-1} , there is a transition and of the experimental data from the linear fit to the data of [PG08].

The shaded area in Fig. 2 indicates the possible error in f for input data with an uncertainty of 10^{-6} with respect to mass density related to the curve of [RM64]). In particular, we conclude that for strongly diluted solutions with $\sigma \rightarrow 0$, it is not possible to experimentally validate or falsify predicted behavior of f .

Dissociation reaction. The net reaction of dissociation and subsequent solvation reaction is written as



where κ_A and κ_C are the numbers of solvent molecules in the solvation shell of A and C, respectively. The stoichiometric coefficients of the reaction are given by ν_A and ν_C on the right hand side of are (75) and

$$\nu_E = -1 , \quad \nu_S = -(\nu_A \kappa_A + \nu_C \kappa_C) \quad (76)$$

taken from the left hand side of (75). We assume that the reaction (75) and the electrolyte in total are electroneutral, viz.

$$z_A N_A + z_C N_C = 0 , \quad z_A \nu_A + z_C \nu_C = 0 . \quad (77)$$

The equilibrium condition for the reaction (75) is according to (13a) given as a mass action law

$$\sum_{\alpha \in \mathcal{I}} \nu_\alpha (\mu_\alpha - g_\alpha^{\text{ref}}) = \Delta g \quad \text{with} \quad \Delta g = - \sum_{\alpha \in \mathcal{I}} \nu_\alpha g_\alpha^{\text{ref}} . \quad (78)$$

If the Gibbs energy Δg is in the order of $+1 \text{ eV}$, then the electrolyte will be effectively completely dissociated up to a certain concentration, depending on the solvation numbers κ_α , where due to a lack of remaining free solvent molecules the solvation of further center ions is not possible any more. For homogeneous systems, the dissociation degree δ is formally introduced such that

$$N_E = (1 - \delta) N_E^0 . \quad (79)$$

In general, the dissociation degree δ is a function of σ . By setting $N_A^0 = N_C^0 = 0$, we have

$$N_\alpha = N_\alpha^0 + \nu_\alpha \delta \sigma N_S^0 \quad \text{for } \alpha \in \mathcal{I} . \quad (80)$$

4.2 Model based determination of δ and f

We define the volume change due to the dissociation reaction as

$$\Delta v(T) := \sum_{\alpha \in \mathcal{I}} \nu_{\alpha} v_{\alpha}^{\text{ref}} \beta_{\alpha}(T) , \quad (81)$$

and introduce the simple mixture reference volume and the according volume factor as

$$V^{\text{sim}} := \sum_{\alpha \in \mathcal{I}} N_{\alpha} v_{\alpha}^{\text{ref}} \beta_{\alpha}(T) , \quad f^{\text{sim}} := \frac{v_E^{\text{ref}} \beta_E^T(T) + \Delta v(T) \delta}{v_S^{\text{ref}} \beta_S(T)} , \quad (82)$$

respectively, such that by applying (80)

$$V^{\text{sim}} = V_S^{\text{ref}} \beta_S \cdot \left(1 + f^{\text{sim}} \sigma \right) , \quad (83)$$

The thermal equation of state (26) can then be rewritten as

$$p^{\text{sim}} = p^{\text{ref}} + K \cdot \left(\frac{1 + f^{\text{sim}} \sigma}{1 + f \sigma} - 1 \right) , \quad (84)$$

In equilibrium, the dissociation reaction satisfies the mass action law (78), and the pressure in the bulk equals the external pressure, see, e.g. [DGM13]. For a given external pressure p^{ref} , the volume of the mixture is determined from

$$p^{\text{ref}} = p , \quad (85a)$$

$$\Delta g = \sum_{\alpha \in \mathcal{I}} \nu_{\alpha} (\mu_{\alpha}^{\text{sim}} - g_{\alpha}^{\text{ref}}) + \sum_{\alpha \in \mathcal{I}} \nu_{\alpha} \mu_{\alpha}^{\text{D}} \quad (85b)$$

Simple mixture of solvated ions at $T = T^{\text{ref}}$. In a first step, we neglect the Debye-Hückel-type energy contributions and only consider the isothermal simple mixture model, i.e. the chemical potentials (32) reduce to

$$\mu_{\alpha} = \mu_{\alpha}^{\text{sim}} = g_{\alpha}^{\text{ref}} + k_B T^{\text{ref}} \ln \left(\frac{n_{\alpha}}{n} \right) + v_{\alpha}^{\text{ref}} K \cdot \ln \left(\sum_{\gamma \in \mathcal{I}} v_{\gamma}^{\text{ref}} n_{\gamma} \right) \quad (86)$$

and pressure satisfies $p = p^{\text{sim}}$. Then, condition (85a) implies $p^{\text{sim}} = p^{\text{ref}}$, i.e. $f = f^{\text{sim}}$ due to (84), what in turn causes the mechanic last contribution in (86) to vanish independently of K . Thus, the mechanic contribution to the law of mass action vanishes completely in (85b) and f and δ can now be determined from

$$f = \frac{v_E^{\text{ref}}}{v_S^{\text{ref}}} + \frac{\Delta v}{v_S^{\text{ref}}} \delta \quad (87a)$$

$$\frac{\Delta g}{k_B T^{\text{ref}}} = \sum_{\alpha \in \mathcal{I}} \nu_{\alpha} \ln \left(\frac{N_{\alpha}}{N} \right) . \quad (87b)$$

Remarkably, (87b) does not depend on the actual volume, or equivalently on f , but only on the dissociation degree δ . However, δ depends on ν_S and thus on the solvation numbers $\kappa_{A/C}$ of the ions. Moreover, $\kappa_{A/C}$ also have an influence on the specific volume $v_{A/C}^{\text{ref}}$ of the solvated ions. If we particularly consider $\nu_A = \nu_C = 1$, then (87b) yields

$$\frac{\Delta g}{k_B T^{\text{ref}}} = \ln \left(\frac{N_A N_C}{N_E N} \left(\frac{N_S}{N} \right)^{\nu_S} \right) = \ln \left(\frac{N_A N_C}{N_E N_S^0} \cdot \frac{N_S^0}{N} \cdot \left(\frac{N_S}{N} \right)^{\nu_S} \right) \quad (88)$$

such that we conclude

$$\exp \left(\frac{\Delta g}{k_B T^{\text{ref}}} \right) = \frac{\delta^2}{1 - \delta} \sigma \frac{1}{1 + (1 + \sum_{\alpha \in \mathcal{I}} \nu_\alpha \delta) \sigma} \left(\frac{1 + (1 + \sum_{\alpha \in \mathcal{I}} \nu_\alpha \delta) \sigma}{1 + \nu_S \delta \sigma} \right)^{-\nu_S}. \quad (89)$$

Without taking the solvation into account, i.e. $\nu_S = \kappa_A + \kappa_C = 0$, the last term of (89) disappears. If we also neglect the second last factor in (89), which approaches unity for small σ , we recover the well known Ostwald's law. The deviation from Ostwald's law and the impact of ion solvation on the dissociation degree are illustrated in Fig. 3. While we do not have direct experimental data for the dissociation degree, we note that within the simple mixture model variations of the volume factor $f = f^{\text{sim}}$ are exclusively due to changes of δ . Thus, in the right plot of Fig. 3 we can also directly observe the impact of the Gibbs energy Δg on the dissociation degree when all particle sizes v_α^{ref} and solvation numbers κ_α are kept fixed. We conclude that within this model already for the parameter value $\Delta g = 0.1 \text{ eV}$ the electrolyte effectively is completely dissociated. For strongly diluted solutions with $\sigma \rightarrow 0$, we have $\delta \rightarrow 1$ and conclude from (82) $f \rightarrow f^0 = \frac{v_E^{\text{ref}} + \Delta v}{v_S^{\text{ref}}}$. We note that all curves $f(\sqrt{\sigma})$ start at $\sigma = 0$ with horizontal slope. Such a horizontal slope is not consistent with a linear law of $f(\sqrt{\sigma})$ according to [RM64]. However, this deviation from the extrapolated linear data fit happens within a region where experimental accuracy is not sufficient to falsify any model hypothesis, cf. Fig. 2. When incomplete dissociation sets in, (87a) shows that the slope of the curves $f(\sigma)$ is proportional to Δv and a fit to experimental data in principle is possible. For the

$$\text{chosen parameters} \quad \Delta g = -0.075 \text{ eV}, \quad \nu_S = \kappa_A + \kappa_C = 12 \quad (90a)$$

$$\text{we obtain from data fit} \quad \Delta v \approx -0.25 v_S^{\text{ref}} \quad v_E^{\text{ref}} + \Delta v \approx 0.95 v_S^{\text{ref}}. \quad (90b)$$

We note that this solution does not require to specify the ion individual parameters of the simple mixture model like v_α^{ref} , κ_α for $\alpha = A, C$, but only combinations thereof.

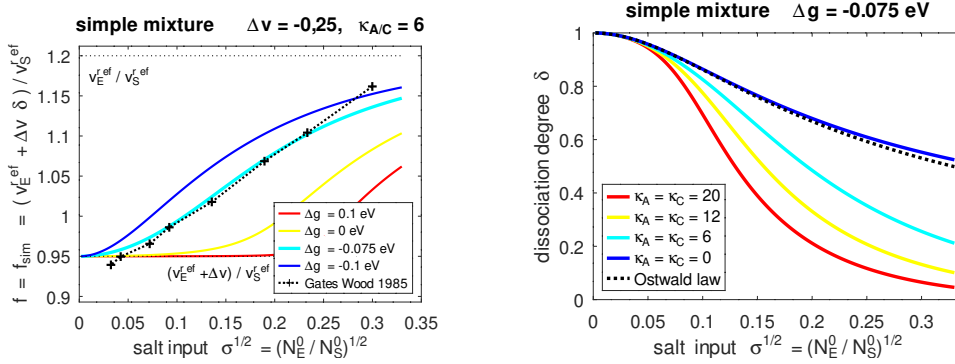


Figure 3: Simple mixture model: Dissociation degree δ decreases more rapid over the salt input σ for larger $\nu_S = \kappa_A + \kappa_C$ (left). Right: Volume change f over the salt input σ for different Δg compared with experimental data of [GW85].

The full model at $T = T^{\text{ref}}$. Compared to the simple mixture, the full model contains the susceptibility χ as additional input data. At $T = T^{\text{ref}}$, we assume for χ the linear relation according to (63a), where the values of the parameters χ_S^{ref} and $d = d_A + d_C$ are given in Table 2. In order to determine the constants χ_α^{ref} , we need to specify d_α , v_α^{ref} and κ_α for $\alpha = A, C$. We choose $\kappa_A = \kappa_C = 6$ and set $d_A = d_{\text{Cl}^-} = 5$, $d_C = d_{\text{Na}^+} = 7$ as suggested by [Mar13]. The resulting values for R_α , v_α^{ref} and χ_α^{ref} for $\alpha \in \{A, C\}$ are listed in Table 4 below. The conditions (85) to determine f and δ read for the full model at $T = T^{\text{ref}}$:

$$-p^{\text{D}} = K \cdot \left(\frac{1 + f^{\text{sim}} \sigma}{1 + f \sigma} - 1 \right), \quad (91a)$$

$$\frac{\Delta g}{k_B T^{\text{ref}}} = \sum_{\alpha \in \mathcal{I}} \nu_\alpha \ln(y_\alpha) + \frac{\Delta v}{k_B T^{\text{ref}}} K \ln \left(1 - \frac{p^{\text{D}}}{K} \right) + \frac{1}{k_B T^{\text{ref}}} \sum_{\alpha \in \mathcal{I}} \nu_\alpha \mu_\alpha^{\text{D}}. \quad (91b)$$

Computed curves of the volume factor $f(\sqrt{\sigma})$ are displayed in Fig. 4 for different values of the Gibbs energy Δg . Since the curves $f(\sqrt{\sigma})$ start with positive slope, the limit value of the volume factor $f^0 = \lim_{\sigma \rightarrow 0} f = (v_E^{\text{ref}} + \Delta v) / v_S^{\text{ref}}$ is lower than in the simple mixture model. The additional pressure contribution p^{D} remains rather small compared to the water bulk modulus K and the upper bound of p^{D} decreases for smaller values of Δg . The curves for the dissociation degree are shown in Fig. 5. For the parameter value $\Delta g = -0.078 \text{ eV}$, there is a non negligibly amount of the undissociated species E present in the electrolyte, although for total salt concentration up to $c = 1 \text{ mol L}^{-1}$ the dissociation degree remains larger than 0.9. Compared to the simple mixture model equipped with the same parameters, the dissociation degree is considerably larger in full model.

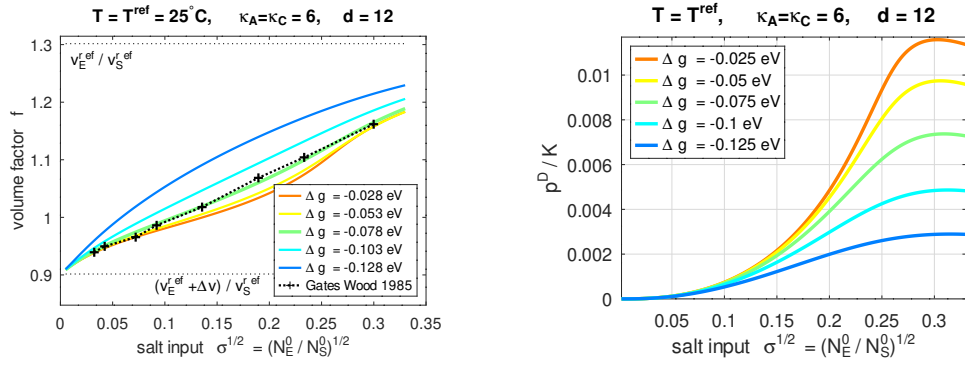


Figure 4: Full model at $T = T^{\text{ref}}$: Computed volume factor f for different values of Δg (left). The pressure contribution p^D is limited to smaller values for more negative Δg (right).

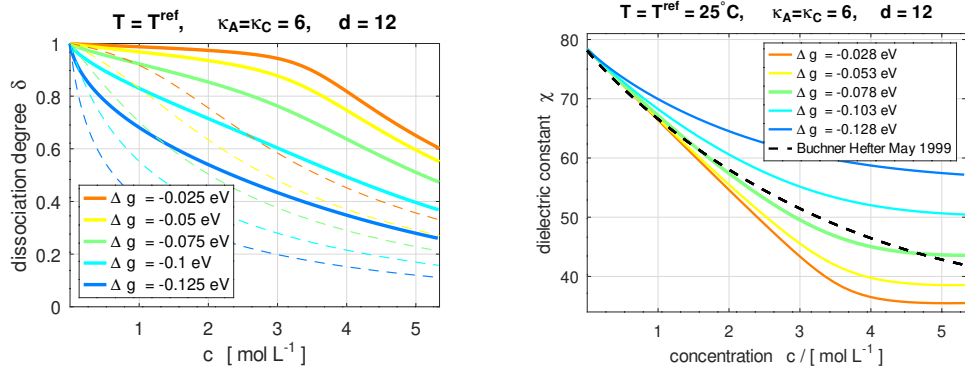


Figure 5: Full model at $T = T^{\text{ref}}$. Left: Computed dissociation degree δ for different values of Δg . For comparison, the dashed lines are related to the simple mixture model. Right: resulting susceptibility χ shows initial linear decrement and later non-linear behavior due to incomplete dissociation.

Due to the assumed linear dependence of the susceptibility on the number densities, there is an impact of the dissociation degree on the computed susceptibility that can be compared with experimental data. For larger values $\Delta g > -0.07$ eV, the curves $\chi(c)$ follow the linear dielectric decrement over a too wide concentration range up to $c \approx 3$ mol L⁻¹ and then rapidly turn into a flat plateau. For smaller values $\Delta g < -0.08$ eV, the curves $\chi(c)$ are too flat and χ does not decrease sufficiently. Moreover, comparison of the computed curves $\chi(c)$ with experimental data from [BHM99] justifies the initial choice $\kappa_A + \kappa_C = 12$, because for values larger than 12, the deviation of $\chi(c)$ from the linear decrement sets in more early and the susceptibility does not decrease sufficiently. To the contrary, for $\kappa_A = \kappa_C = 5$, the linear decrement holds for a too wide range of salt concentrations. We note that the thus far unspecified remaining parameter χ_E^{ref} only has a minor impact on the overall solution of (91) that mainly can be observed in $\chi(c)$ for large concentrations $c > 4$ mol L⁻¹. For the computations, we made the rather arbitrary choice $\chi_E^{\text{ref}} = (\chi_A^{\text{ref}} + \chi_C^{\text{ref}})/2$.

Temperatures $T \neq T^{\text{ref}}$. In order to compute the volume factor at temperatures $T \neq T^{\text{ref}}$, the thermal expansion coefficients $\beta_\alpha(T)$ need to be specified. We choose $\beta_S(T)$ according to the data for water in [AM99]. Since we are not aware of any thermal expansion data for solvated ions, we apply linearization at T^{ref} with the coefficients $\beta_A^{\text{ref}}, \beta_C^{\text{ref}}$ as in Table 4. Due to its minor impact on the computed results, we set the coefficient for the undissociated species E to coincide at $T = T^{\text{ref}}$ with the slope of $\beta_S(T^{\text{ref}})$, i.e. $\beta_E^{\text{ref}} = 255.75 \cdot 10^{-6}$. For the evaluation of the functions $F(R_\alpha, \lambda)$, the radii R_α at the temperature T have to be determined in accordance with the thermal expansion. Moreover, the potentials μ_α^{D} , as well as the pressure contribution p^{D} contain derivatives $\frac{\partial}{\partial n_\alpha} \chi$, which are a-priori unknown for $T \neq T^{\text{ref}}$ and have to be determined such that (50) is satisfied. Therefore, we verify

$$\begin{aligned} & \frac{\partial}{\partial n_\alpha} \left(\left(\frac{\chi}{D} \right)^2 \sum_{\gamma \in \mathcal{I}} z_\gamma^2 \frac{n_\gamma}{n^{\text{ref}}} F(R_\gamma, \lambda) \right) \\ &= \frac{\partial}{\partial n_\alpha} \chi \sum_{\gamma \in \mathcal{I}} z_\gamma^2 \frac{n_\gamma}{n^{\text{ref}}} \left(\frac{\chi}{D^3} F(R_\gamma, \lambda) - \frac{\chi^2}{D^3} \frac{\lambda}{2} F'(R_\gamma, \lambda) \right) \\ & \quad + \frac{\chi^2}{D^2} \frac{z_\alpha^2}{\tau D \lambda^2} \sum_{\gamma \in \mathcal{I}} z_\gamma^2 \frac{n_\gamma}{n^{\text{ref}}} \frac{\lambda}{2} F'(R_\gamma, \lambda) + \frac{\chi^2}{D^2} \frac{z_\alpha^2}{n^{\text{ref}}} F(R_\alpha, \lambda) . \end{aligned} \quad (92)$$

Then, we take the derivative of (64) with respect to n_α , where on the right hand side we evaluate (92) for $T = T^{\text{ref}}$, to finally determine $\frac{\partial}{\partial n_\alpha} \chi$ for $T \neq T^{\text{ref}}$.

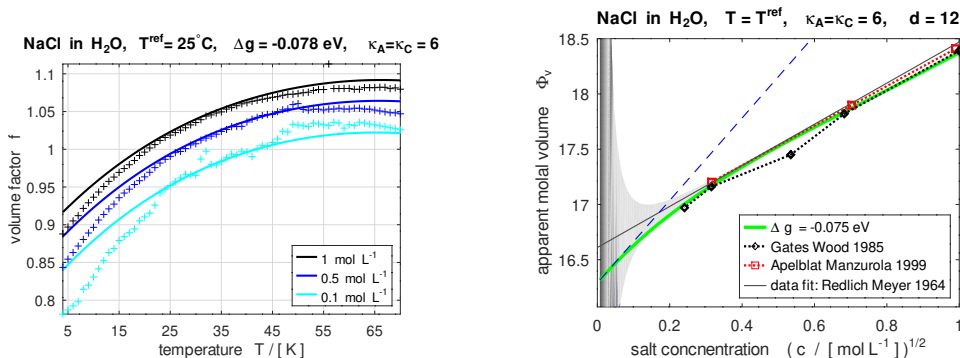


Figure 6: Left: Computed volume factor $f(T)$ for solutions of different molality (solid lines) and experimental data of [AM99] (crosses). Right: The limiting slope according to (100)

The computed volume factor $f(T)$ as a function of temperature is shown in Fig. 6 for different solutions of fixed salt molality. Due to the linearization of the thermal expansion coefficients, the accuracy of the computed curves is limited to a vicinity around the reference temperature with a width in the order of 10 K. More results, showing the concentration and temperature dependence of the apparent molar volume, are presented below on Sect. 4.4.

4.3 Limiting slopes for strong dilution

The results of Debye-Hückel theory are most often expressed in the form of limiting laws for $\sigma \rightarrow 0$. An empirical limit law for the molal volume at infinite dilution was proposed by Masson [Mas29], viz.

$$\Phi_V = \Phi_V^0 + S_V \sqrt{c}, \quad (93)$$

with individual slopes S_V for each electrolyte. A formally identic equation was derived by Redlich and Rosenfeld from an extension of [DH23a] with temperature dependent susceptibility [RR31]. There, the slope is of the form $S_V = k \sqrt{w^3}$, where w is a factor depending only on the valency of the ions and k uniquely determined by the Debye-Hückel theory. Based on later experimental data, the parameters were identified as $\Phi_V^0 \approx 16.61$ and $S_V \approx 1.86$, cf. [RM64]. The discrepancy between these theoretical values and the empirical slopes related to the Masson equation caused a controversy that was resolved in such a way, cf. [RM64, Mil71] that the theoretical equation by [RR31] is considered valid, although possibly only for ion concentrations that are too low to allow accurate measurements, whereas the empirical equation is also valid but in an electrolyte concentration range where ion specific effects already caused deviations from the Debye-Hückel type limiting law.

To determine the limit slope of the volume factor f in the strong dilution limit, we start from (85a) that we rearrange as

$$f = \frac{\frac{p^D}{\sigma} + K f^{\text{sim}}}{K - p^D} . \quad (94)$$

Then, we check $\lim_{\sigma \rightarrow 0} n_\alpha = 0$ for $\alpha \in \{A, C, E\}$, $\lim_{\sigma \rightarrow 0} \delta = 1$, $\lim_{\sigma \rightarrow 0} \chi = \chi_S^{\text{ref}}$, $\lim_{\sigma \rightarrow 0} p^D = 0$ and $\lim_{\sigma \rightarrow 0} \partial_{\sqrt{\sigma}} p^D = 0$, to infer

$$\lim_{\sigma \rightarrow 0} \partial_{\sqrt{\sigma}} f = \lim_{\sigma \rightarrow 0} \left(\frac{\partial_{\sqrt{\sigma}} \left(\frac{p^D}{\sigma} \right)}{K - p^D} + \frac{\frac{p^D}{K} + K f^{\text{sim}}}{(K - p^D)^2} \partial_{\sqrt{\sigma}} p^D \right) = \lim_{\sigma \rightarrow 0} \frac{\partial_{\sqrt{\sigma}} \left(\frac{p^D}{\sigma} \right)}{K} . \quad (95)$$

We abbreviate $F'_\gamma = \frac{\partial}{\partial \lambda} F(R_\gamma, \lambda)$. With $\lim_{\sigma \rightarrow 0} \lambda = 0$, we deduce $\lim_{\sigma \rightarrow 0} F(R_\gamma, \lambda) = \lim_{\sigma \rightarrow 0} (\lambda F'_\gamma) = 0$. Dividing the pressure contribution p^D from (54c) by σ and applying product rule shows that the remaining non-vanishing terms in (95) in the limit $\sigma \rightarrow 0$ are

$$\lim_{\sigma \rightarrow 0} \partial_{\sqrt{\sigma}} f = -\frac{a}{2K} \frac{\chi_S^{\text{ref}}}{(1 + \chi_S^{\text{ref}})^2} \sum_{\beta \in \{A, C\}} z_\gamma^2 \lim_{\sigma \rightarrow 0} \left(\frac{n_\gamma}{n^{\text{ref}} \sigma} \cdot \partial_{\sqrt{\sigma}} \lambda \right) \times \quad (96)$$

$$\lim_{\sigma \rightarrow 0} \partial_\lambda \left[\frac{\lambda}{2} F'_\gamma(R_\gamma, \lambda) \frac{1 + \chi - \mathcal{L}_\chi}{1 + \chi} - F(R_\gamma, \lambda) \frac{\chi - 1}{1 + \chi} \frac{\mathcal{L}_\chi}{\chi} \right] .$$

Applying again product rule in (96) and going to the limit $\sigma \rightarrow 0$, the only non-vanishing terms in the square brackets are

$$\lim_{\sigma \rightarrow 0} \partial_\lambda \left[\frac{\lambda}{2} F'_\gamma \cdot (1 + \chi - \mathcal{L}_\chi) - F(R_\gamma, \lambda) (\chi - 1) \frac{\mathcal{L}_\chi}{\chi} \right] = \left[\frac{1}{2} \lim_{\sigma \rightarrow 0} F'_\gamma - (\chi_S^{\text{ref}} - 1) \lim_{\sigma \rightarrow 0} F'_\gamma \right] \quad (97)$$

We check that in the limit $\sigma \rightarrow 0$ we have the identities

$$\lim_{\sigma \rightarrow 0} \frac{n_\gamma}{\sigma} = \lim_{\sigma \rightarrow 0} \frac{\nu_\gamma \delta N_S^0}{V_S^{\text{ref}} (1 + f\sigma)} = \frac{\nu_\gamma}{v_S^{\text{ref}}} , \quad (98a)$$

$$\lim_{\sigma \rightarrow 0} \partial_{\sqrt{\sigma}} \lambda = \frac{1}{\sqrt{(1 + \chi_S^{\text{ref}}) \tau}} \sqrt{\sum_{\beta \in \{A, C\}} \frac{\nu_\gamma z_\gamma^2}{v_S^{\text{ref}} n^{\text{ref}}}} , \quad (98b)$$

to conclude that the limit slope for the volume factor is

$$\lim_{\sigma \rightarrow 0} \partial_{\sqrt{\sigma}} f = \frac{a}{4K} \frac{\chi_S^{\text{ref}}}{(1 + \chi_S^{\text{ref}})^3} \frac{(2\chi_S^{\text{ref}} - 3) F'_0}{\sqrt{(1 + \chi_S^{\text{ref}}) \tau}} \sqrt{\sum_{\beta \in \{A, C\}} \frac{\nu_\gamma z_\gamma^2}{v_S^{\text{ref}} n^{\text{ref}}}} , \quad (99)$$

where F'_0 denotes the unique limit $\lim_{\lambda \rightarrow 0} F'_\gamma$ for all $\gamma \in \mathcal{I}$. This limit slope has the same structure $\lim_{\sigma \rightarrow 0} \partial_{\sqrt{\sigma}} f = S_f = k_f \sqrt{w_f}^3$ as the above mentioned slope derived by [RR31]. The numeric value of the limit slope is then obtained from

$$\lim_{\sigma \rightarrow 0} F'(R_\gamma, \lambda) = \lim_{\sigma \rightarrow 0} \left(\frac{3 + 4\lambda R_\alpha / \ell}{(1 + \lambda R_\alpha / \ell)^2} - 2\lambda R_\alpha / \ell \frac{3 + 2\lambda R_\alpha / \ell}{(1 + \lambda R_\alpha / \ell)^3} \right) = 3. \quad (100)$$

For the apparent molar volume, we thus get a limit slope $S_V = 3.7306$, approximately twice of the value by [RR31]. The computed apparent molar volume in the dilute regime, together with experimental data and the limit law according to [RM64], are displayed in Fig. 6. We observe, that the limit law only holds for rather low concentrations up to ca. 0.05 mol L^{-1} and the deviation with respect to the standard Debye-Hückel limit according to [RR31, RM64] is within the shaded region indicating an uncertainty in the underlying mass density of the solution less than $2.5 \cdot 10^{-6} \text{ kg L}^{-1}$. Since the here computed molar volume has a steeper slope for $c \rightarrow 0$, the apparent volume at infinite dilution $\Phi_V^0 = \lim_{c \rightarrow 0} \Phi_V = 16.2904$ is smaller than 16.61 according to [RM64].

4.4 Application to different salts and various temperatures

So far, we computed the volume factor f , or the equivalent apparent molar volume Φ_V , using one set of parameters. However, going from one salt to another related salt, sharing either the same anion or the same cation, the model parameters can not be chosen completely independently. None of the model parameters for solvated ions, i.e. $v_\alpha^{\text{ref}}, \chi_\alpha^{\text{ref}}$ for $\alpha \in \{A, C\}$, is directly available from experimental data. In addition also parameters κ_α and the Gibbs energy Δg of the dissociation reaction are needed. Table 3 lists parameter values that can be deduced from experimental data. Here, the values for the dielectric decrement d are based on [Mar13]. The values for the molar volume at infinite dilution Φ_V^0 and for the volume change Δv are based on [PDH84] for the fluoride salts, [GW85] for the chloride salts and [HLLH16, HH21] for the perchlorate salts.

The definition (81) together with $f^0 v_S^{\text{ref}} = v_E^{\text{ref}} + \Delta v$ yield the relation

$$v_A^{\text{ref}} + v_C^{\text{ref}} = (f^0 + \kappa_A + \kappa_C) v_S^{\text{ref}} \quad (101)$$

that determines the difference in f^0 when exchanging one ion with another. An analogous relation for the bare, unsolvated ions has been used to define *conventional partial molar volumes* relative to the H^+ ion as a reference, cf. [Mil71, Mar11]. Due to singularity of experimental uncertainty, values Φ_V^0 necessarily have to rely on extrapolation of data and thus depend on the assumed theoretical model. Since the model proposed here differs in

Table 3: Salt specific parameters for aqueous solutions deduced from experimental data at the reference temperature $T^{\text{ref}} = 25^\circ\text{C}$.

	LiF	NaF	KF	LiCl	NaCl	KCl	LiClO ₄	NaClO ₄	KClO ₄
f^0	-0.149	-0.168	0.397	0.921	0.902	1.47	2.37	2.35	2.92
$\Rightarrow \Phi_V^0$	-2.684	-3.04	7.18	16.65	16.29	26.51	42.89	42.53	52.75
$\Delta v/v_S^{\text{ref}}$	-2.05	-0.5	-0.6	-0.2	-0.4	-0.5	-0.1	-0.35	-0.2
d	13	12	11	13	12	11	15	14	13
$\Delta g/[\text{eV}]$	-0.1	-0.105	-0.085	-0.7	-0.78	-0.8	-0.1	-0.085	-0.14

the limiting behavior from the standard Debye-Hückel theory, the obtained values of Φ_V^0 also differ from those found in the literature. However, instead of relative partial apparent molar volumes, our model requires as parameters absolute specific volumes v_α^{ref} of solvated ions and the related assigned radii R_α . Therefore, a suitable choice for v_α^{ref} and κ_α needs to be done in order to let (101) approximate the f^0 data of Tab.3. We keep the above choice $\kappa_\alpha = 6$ and the chosen values of v_α^{ref} are listed in Tab. 4, together with the related radii R_α of the solvated ions and \tilde{r}_α of the unsolvated center ions according to

$$R_\alpha = \sqrt[3]{\frac{3}{4\pi} \cdot v_\alpha^{\text{ref}} \beta_\alpha}, \quad \tilde{r}_\alpha = \sqrt[3]{\frac{3}{4\pi} \cdot (v_\alpha^{\text{ref}} \beta_\alpha - (\kappa_\alpha v_S^{\text{ref}} \beta_S))}. \quad (102)$$

The limiting molar volume at infinite dilution can be small, or even negative, e.g. in the case of LiF or NaF dissolved in water. Thus, the specific volume v_α^{ref} can be smaller than the sum of κ_α solvent molecules. Hence, while v_α^{ref} always has to be positive, the radius \tilde{r}_α in general can also be negative, cf. \tilde{r}_F in Tab. 4.

The parameters for the linearized thermal expansion coefficients are chosen based on [AM99, HH21] for Na^+ , K^+ , Cl^- and ClO_4^- , [AM01, HHLH16] for Li^+ and [MDH68] for F^- , whereas the coefficient for the undissociated salt in the following is in all cases set to the arbitrary value $\beta_E^{\text{ref}} = 255.75 \cdot 10^{-6}$ corresponding to the thermal expansion of water at $T = 25^\circ\text{C}$.

The apparent molar volume as function of the salt concentration and for different temperatures was computed for the set of related salts NaCl, KCl, NaClO₄ and KClO₄. The parameters specific to the ions were set as in Table 4. In addition there are parameters specific to each salt. These are the specific volume v_E^{ref} that follows from f^0 and Δv listed in Table 4 and susceptibility coefficient χ_E^{ref} and the Gibbs energy energy Δg of the dissociation reaction. The value $\Delta g_{\text{NaCl}} = -0.78 \text{ eV}$ was checked against concentration dependent susceptibility data of [BHM99] and $\Delta g_{\text{KCl}} = -0.1 \text{ eV}$ based on susceptibility data of [CHB03]. Moreover, we set $\Delta g = -0.1 \text{ eV}$ for the perchlorate salts. The coefficients χ_E^{ref} were arbitrarily set to $\chi_E^{\text{ref}} = (\chi_A^{\text{ref}} + \chi_C^{\text{ref}})/2$. Computed

Table 4: Ion specific parameters at $T^{\text{ref}} = 25^\circ\text{C}$ based on the choice $\kappa_\alpha = 6$: specific volumes v_α^{ref} and the implied radii R_α of the solvated ion and \tilde{r}_α associated with the unsolvated ion in solution, additive dielectric decrement d_α and $\beta_\alpha^{\text{ref}}$ for the linearization of the thermal expansion at $T = T^{\text{ref}}$.

	Li ⁺	Na ⁺	K ⁺	F ⁻	Cl ⁻	ClO ₄ ⁻
$v_\alpha^{\text{ref}} 1000\mathcal{N}_A / [\text{L mol}^{-1}]$	0.12276	0.1224	0.13262	0.09138	0.11071	0.13695
$\Rightarrow R_\alpha/\ell$	7.5189	7.5116	7.7151	6.8144	7.2645	7.7983
$\Rightarrow \tilde{r}_\alpha / [\text{pm}]$	178.5	177	212.5	-189	97	224.5
d_α	8	7	6	5	5	7
$\Rightarrow \chi_\alpha^{\text{ref}}$	13.21	21.19	33.14	23.66	33.22	27.27
$\beta_\alpha^{\text{ref}} \cdot 10^6$	306.9	754.5	690.5	306.9	319.7	1074.2

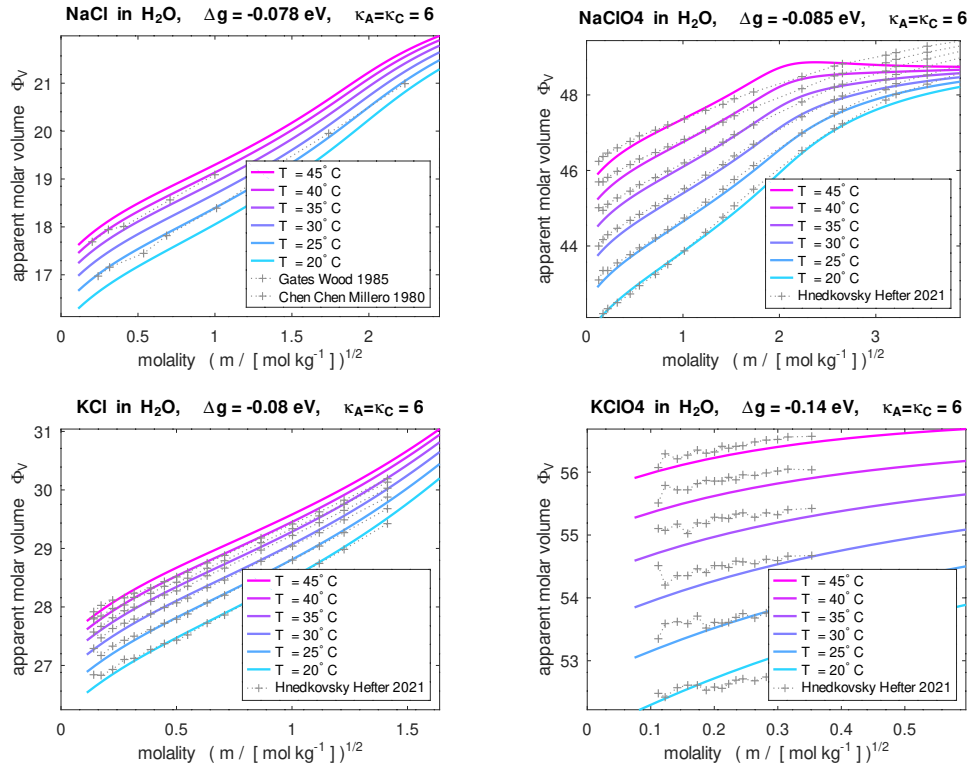


Figure 7: Apparent molar volume for the related salts NaCl, KCl, NaClO₄ and KClO₄ computed from a single set of parameters as given in Tab. 4 and experimental data for comparison.

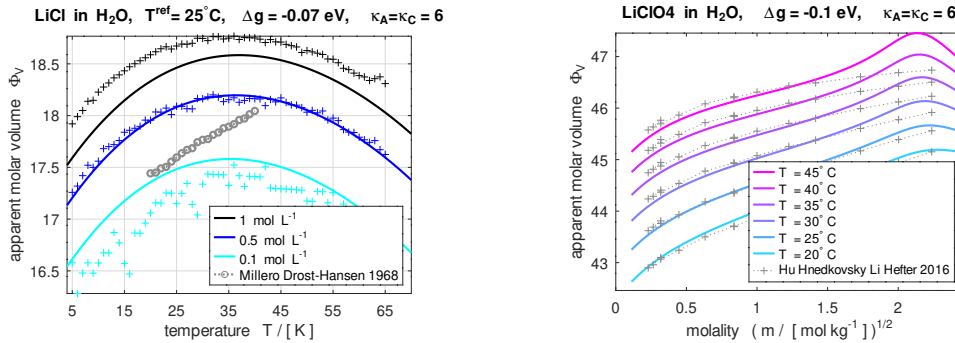


Figure 8: Left: Computed apparent molal volume of LiCl solutions of fixed concentration (solid lines) show a local maximum at $T \approx 40^\circ\text{C}$ like experimentally observed in [AM01] (marker). Right: Computed apparent molal volume of aqueous LiClO₄ solutions and data of [HHLH16] for comparison.

curves and good agreement with experimental data of [AW81, HHLH16, HH21] are shown in Fig. 7.

More related salts can be considered sharing the Li⁺ cation. As stated in [AM01], their data confirms earlier observations [Ell66, HO59] that aqueous LiCl solutions show a local maximum of the apparent molar volume near $T \approx 40^\circ\text{C}$, much earlier than for solutions of NaCl or KCl, where the maximum occurs around $T \approx 60^\circ\text{C}$. Remarkably, this maximum is well captured by the computed curves for LiCl in Fig. 8, whereas because of the large difference to the reference temperature for linearization the computed apparent molar volume does not reproduce the local maximum for NaCl, cf. Fig. 6, or similarly also for KCl. Here, the Gibbs energy $\Delta g_{\text{LiCl}} = -0.095\text{ eV}$ was adjusted according to [GW85] at 25°C . As pointed out in [AM01], their measured values for small molality 0.1 mol L^{-1} are low compared to e.g. [GW85] at 25°C or [MDH68] for a slightly higher molality.

The apparent molar volume of LiClO₄ in aqueous solutions as a function of temperature and molality can be computed with the parameters fixed so far and $\Delta g_{\text{LiClO}_4} = -0.1\text{ eV}$ to reach good agreement with the experimental data of [HHLH16].

5 Application to phase boundaries of binary electrolytes

We consider a planar interface, where on the one side there is only the pure solvent S present and on the other side of the surface, there is a liquid electrolytic mixture consisting of the species $\{A, C, E, S\}$. For the pure solvent, we denote the Gibbs energy by $g_S^{\text{pure}}(T, p)$. In the other subdomain, the electrochemical potentials are constant in equilibrium. Since we assume

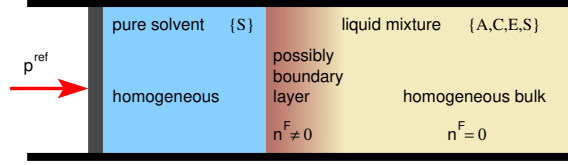


Figure 9: Interface between pure solvent (solid or gas) and liquid mixture with possibly a charged boundary layer in the mixture.

the solvent S electrically neutral, the chemical potential μ_S is constant within the whole subdomain of the mixture, even in the presence of a charged boundary layer at the surface.

Both phases are in equilibrium, if

$$g_S^{\text{pure}} \stackrel{!}{=} \mu_S . \quad (103)$$

In the mixture, we introduce

$$g_\alpha(T, p) = g_\alpha^{\text{ref}} + m_\alpha c_\alpha^{\text{ref}} \cdot \left(T - T^{\text{ref}} - T \ln \left(\frac{T}{T^{\text{ref}}} \right) \right) - m_\alpha s_\alpha^{\text{ref}} \cdot (T - T^{\text{ref}}) \\ + v_\alpha^{\text{ref}} \beta_\alpha(T) (p - p^{\text{ref}}) + v_\alpha^{\text{ref}} (\beta_\alpha(T) - 1) p^{\text{ref}} . \quad (104)$$

Then, we apply the thermal equation of state from (56) to the chemical potential of the solvent and employ linearization of the logarithm of the pressure for large bulk modulus K , such that

$$\mu_S = g_S(T, p^{\text{ref}}) + v_S^{\text{ref}} \beta_S(T) \cdot (p - p^{\text{ref}}) + k_B T \ln(y_S) + \mu_S^{\text{D}} - v_S^{\text{ref}} \beta_S(T) \cdot p^{\text{D}} . \quad (105)$$

In the particular case that there is only the solvent present on both of the interface, but possibly in different phases, there holds

$$\underline{y_S = 1}: \quad g_S^{\text{pure}}(T, p) \stackrel{!}{=} g_S(T, p) . \quad (106)$$

When the pressure in the subdomain of the pure phase is controlled, then solution of (106) defines either the *melting temperature* $T^S(p)$ or the *boiling temperature* $T^V(p)$ of the solvent, respectively, depending on whether the pure phase is solid or vapour state. On the other hand, we may alternatively control the temperature in the pure phase. Then, solution of (106) defines the *vapour pressure* $p^V(T)$.

In the oversimplified ideal gas analogy of the early electrolyte theory, the phase boundary was associated with a semipermeable membrane and the phase equilibrium (103) was used to introduce the notion of an 'osmotic pressure'. Such an 'osmotic pressure' cannot be reconciled with the very precisely defined concept of pressure within the applied electro-thermodynamic

framework employed here. And since real semipermeable membranes cannot provide reproducible results in practice, they are also not suitable for testing a theory. However, there is the commonly used quantity called '*osmotic coefficient*', defined as

$$\phi = -\frac{\mu_S - g_S(T, p^{\text{ref}})}{k_B T (\nu_A + \nu_C) m_S \mathcal{N}_A \cdot m}, \quad (107)$$

which can serve as some kind of measure to compare the results obtained from the here proposed model to results found in the literature. Measurements of vapour pressure, freezing point depression and boiling point elevation can be used to determine the '*osmotic coefficient*'.

5.1 Reduction of vapour pressure

We assume that the pure solvent side is in vapour phase and that it can be treated as an ideal gas such that the Gibbs energy of the pure solvent is

$$g_S^{\text{pure}}(T, p) = g_S(T, p^V(T)) + k_B T \ln \left(\frac{p}{p^V(T)} \right). \quad (108)$$

Then, the equilibrium condition (103) reads

$$\ln \left(\frac{p}{p^V(T)} \right) = \frac{v_S^{\text{ref}} \beta_S(T)}{k_B T} (p^{\text{ref}} - p^V(T)) + \frac{\mu_S - g_S(T, p^{\text{ref}})}{k_B T}. \quad (109)$$

On the vapour side, the ideal gas law defines the specific volume v_S^V by $p^V(T) \cdot v_S^V = k_B T$, where $p^V(T)$ be the vapour pressure of the solvent determined by (106) at temperature T . Thus,

$$\ln \left(\frac{p}{p^V(T)} \right) = \left(\frac{p^{\text{ref}}}{p^V(T)} - 1 \right) \frac{v_S^{\text{ref}} \beta_S(T)}{v_S^V} - \phi \cdot (\nu_A + \nu_C) m_S \mathcal{N}_A \cdot m. \quad (110)$$

For water at temperatures near 25°C , the first term on the right hand side is small because $v_S^{\text{ref}} \approx 2.3 \cdot 10^{-5} v_S^V$ and can be neglected. We thus conclude that the vapour pressure of the electrolytic mixture is

$$\frac{p}{p^V(T)} = \exp \left(-\phi \cdot (\nu_A + \nu_C) m_S \mathcal{N}_A \cdot m \right). \quad (111)$$

To compute the vapour pressure of an aqueous NaCl solution, we set $T^{\text{ref}} = 25^\circ\text{C}$ and p^{ref} equal to atmospheric pressure and use the same set of model parameters that have been employed before in Sect. 4, cf. Tables 2-4. For the vapour pressure of pure water, we used the values given in [Lid05, Tab. 6-8]. The results are shown in Fig. 10 and compared with experimental data [PD72, HGBS95] and tabulated values based on a regression model [CG85]. We observe that the computed vapour pressure

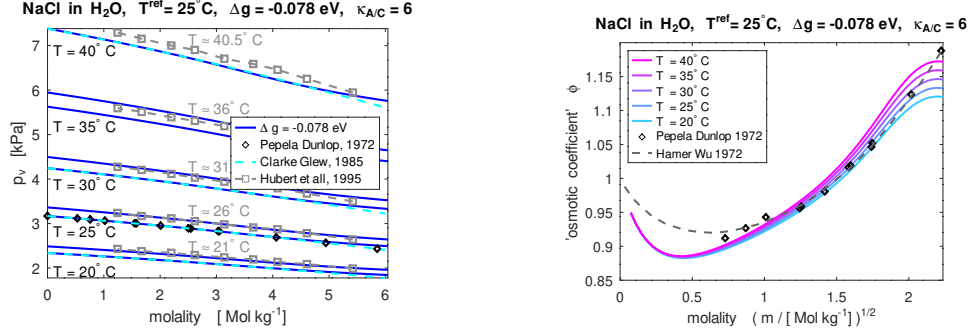


Figure 10: Left: Computed concentration dependent vapour pressure for different temperatures T follows the literature data [PD72, CG85, HG85] closely up to 5 mol L^{-1} . Right: 'Osmotic coefficient' based on the complete model shows weak temperature dependence for higher salt concentrations. For comparison 'osmotic coefficient' derived from vapour pressure data [PD72] at $T = 25^\circ\text{C}$ and reference data from [HW72].

follows the experimental results very closely over the whole tested temperature and concentration range, although the model parameters have been chosen on the basis of different independent experiments, i.e. apparent molar volume and concentration dependent susceptibility. The 'osmotic coefficients' based on our model show at higher salt concentrations some temperature dependence that vanishes for strongly diluted solutions. The 'osmotic coefficients' derived from vapour pressure measurements [PD72] at $T = 25^\circ\text{C}$ agree well with the computed curves. For low concentrations, where we have no data from vapour pressure measurements, the reference data [HW72] based on a regression model incorporating the Debye-Hückel theory shows some deviations to the results of our model. In comparison, our model yields a steeper slope in the limit of infinite dilution and has an earlier and deeper local minimum.

5.2 Freezing point depression at $p = p^{\text{ref}}$

We consider the pure solvent in solid phase and fix the pressure in this subdomain to the reference pressure p^{ref} such that T^S is given by solution of (106) with $p = p^{\text{ref}}$. For the freezing point of water at atmospheric pressure, we have $T^S = 273.15 \text{ K}$. Applying (105) with $p = p^{\text{ref}}$ to the equilibrium condition (103) yields

$$g_S^{\text{pure}}(T, p^{\text{ref}}) = g_S(T, p^{\text{ref}}) + k_B T \ln(y_S) + \mu_S^{\text{D}} - v_S^{\text{ref}} \beta_S(T) \cdot p^{\text{D}}. \quad (112)$$

We linearize g_S and g_S^{pure} around the state (T^S, p^{ref}) . Therefore, we introduce

$$\Delta := T^S - T, \quad s := -\partial_T g_S(T^S, p^{\text{ref}}), \quad s^{\text{pure}} := -\partial_T g_S^{\text{pure}}(T^S, p^{\text{ref}}). \quad (113)$$

With (106) and linearization of the thermal expansion $\beta_\alpha \approx 1 - \beta_\alpha^{\text{ref}} \cdot \Delta$, we infer

$$g_S^{\text{pure}}(T, p^{\text{ref}}) - g_S(T, p^{\text{ref}}) = (s^{\text{pure}} - s) \Delta + \mathcal{O}(\Delta^2), \quad (114a)$$

such that neglecting the higher order terms we get from (112)

$$(s^{\text{pure}} - s) \Delta = k_B T \ln(y_S) + \mu_S^{\text{D}} - v_S^{\text{ref}} \beta_S(T) p^{\text{D}}. \quad (115)$$

With the enthalpy of fusion $-q = \frac{T^S}{m_S}(s^{\text{pure}} - s)$, (107) and (73b) the lowering of the freezing point Δ is determined by

$$\begin{aligned} -\frac{m_S}{k_B T} q \frac{\Delta}{T^S} &= \ln(y_S) + \frac{\mu_S^{\text{D}} - v_S^{\text{ref}} \beta_S(T) p^{\text{D}}}{k_B T} \\ &= -\phi \cdot 1000 \mathcal{N}_A v_S^{\text{ref}} \beta_S(T) (1 + f\sigma)(\nu_A + \nu_C) \cdot c. \end{aligned} \quad (116)$$

Simple mixture and classical limit. In the simple mixture model, the contributions from the electric interaction disappear in (116). For comparison with the full model, we introduce Δ_{sim} defined as

$$-\frac{m_S}{k_B T} q \frac{\Delta_{\text{sim}}}{T^S} = \ln(y_S). \quad (117)$$

In the limit of strong dilution the simple mixture approaches the standard ideal electrolyte theory, i.e. we can assume complete dissociation and $n_\alpha \ll n_S$ for $\alpha \in \{A, C\}$, such that $v_S^{\text{ref}} \beta_S(T) n_S \approx 1$. Then, we approximate $\ln(y_S) \approx -\sum_{\alpha \neq S} \frac{n_\alpha}{n_S}$. The ideal electrolyte limit of (117) thus reads

$$\Delta_{\text{ideal}} = T^S \frac{k_B T}{m_S q} v_S^{\text{ref}} \beta_S(T) \sum_{\alpha \in \{A, C\}} n_\alpha \quad (118)$$

When we express the ionic number densities in terms of the concentration in mol L^{-1} as $n_A + n_C = (\nu_A + \nu_C) \cdot 1000 \mathcal{N}_A \cdot c$, we can conclude the relations

$$\frac{\Delta}{\Delta_{\text{ideal}}} = (1 + f\sigma) \cdot \phi, \quad \Delta_{\text{ideal}} \approx 1.8623 \frac{\text{K L}}{\text{mol}} \cdot 2c, \quad (119)$$

where we used $q \approx 333.55 \text{ J g}^{-1}$ for water at atmospheric pressure p^{ref} and approximated $T \approx T^S$.

Comparison to experiments. When computing the freezing point depression Δ and 'osmotic coefficient' ϕ , we have to apply model parameters different than in Sect. 4, in order to account for the reference temperature $T^{\text{ref}} = T^S = 0^\circ\text{C}$. We set $v_S^{\text{ref}} = (55.5 \cdot n^{\text{ref}})^{-1}$ and $d_A = 6$ and $d_C = 8$ to achieve $d = d_A + d_C = 14$ as motivated by data of [BHM99] for 5°C . Using the density data of [CCM80], and with $\Delta g = -0.78 \text{ eV}$, we adjust

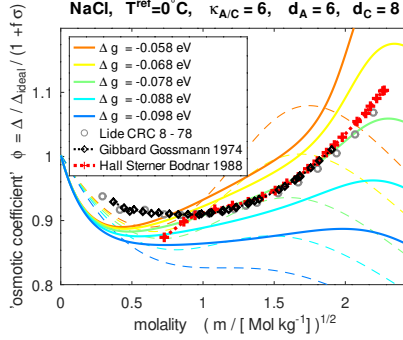


Figure 11: Left: Computed 'osmotic coefficient' derived from freezing point depression for different values of Δg and comparison with data from [Lid05, GG74, HSB88]. The dashed lines are related to the Debye-Hückel energy of [DH23a].

the size parameters of the ionic species to $\tilde{r}_A = 82$ pm and $\tilde{r}_C = 163$ pm and set $\Delta v = -0.9$. For simplicity, we evaluated (116) at T^S instead of T . Fig. 11 shows that the computed 'osmotic coefficient' for different values of the Gibbs energy Δg . We observe that the curve agrees best with the experimental data for $m \geq 1$ mol L $^{-1}$ for the same $\Delta g = -0.78$ eV that also matched the computed apparent molar volume to the mass density data of [CCM80]. For molality less than $m \leq 1$ mol L $^{-1}$, there is a visible deviation between the experimental data and the computed curves. This appears to be caused by the rather steep slope in the beginning of the curves and the local minimum that is approached early. The dashed lines in Fig. 11 show for comparison also the computed 'osmotic coefficient' from the simple mixture with the original Debye-Hückel energy added. From the experimental data, no conclusions about the correct limit slope can be drawn and for $m \approx 0.2$ mol L $^{-1}$ the distance of both sets of computed curves to the experimental data is comparable in size. Remarkably, there is a gap between the different experimental data, which opens up at $m \approx 0.8$ mol L $^{-1}$ and encloses the computed curves.

Limiting law. To analyze the freezing point depression in the limit $c \rightarrow 0$, we first check on the left hand side of (116) that

$$\mu_S^D - v_S^{\text{ref}} p^D = + \frac{a}{2} \frac{\chi}{D^2} \left(v_S^{\text{ref}} \beta_S(T) \frac{\lambda}{2} d\mathcal{F} - \left(\frac{\chi - 1}{\chi} \mathcal{F} + \frac{\lambda}{2} d\mathcal{F} \right) \frac{v_S^{\text{ref}} \beta_S(T) \mathcal{L}_\chi - \frac{\partial}{\partial n_S} \chi}{D} \right). \quad (120)$$

For a strongly diluted solution we may assume $1 + f\sigma \rightarrow 1$, as well as $v_S^{\text{ref}} \beta_S(T) \mathcal{L}_\chi = v_S^{\text{ref}} \beta_S(T) \sum_{\gamma \in \mathcal{I}} n_\gamma \frac{\partial}{\partial n_\gamma} \chi \rightarrow \frac{\partial}{\partial n_S} \chi$. We thus approximate

(116) as

$$-\frac{m_S}{k_B T^S} q \frac{\Delta}{T} = \ln(y_S) + \frac{a v_S^{\text{ref}} \beta_S(T)}{4 k_B T} \frac{\chi}{D^2} \lambda d\mathcal{F}. \quad (121)$$

Subtracting from this the simple mixture relation (117) and applying the strong dilution limit (118), the difference of the full model to the standard ideal theory can be expressed as

$$\begin{aligned} \frac{\Delta_{\text{sim}} - \Delta}{\Delta_{\text{ideal}}} &= \frac{1}{\Delta_{\text{ideal}}} \frac{T^S}{m_S q} \frac{a v_S^{\text{ref}} \beta_S(T)}{4} \frac{\chi}{D^2} \lambda d\mathcal{F} \\ &= \frac{a}{4 k_B T} \frac{\ell}{n^{\text{ref}}} \frac{\chi}{D^2} \Lambda \frac{\sum_{\alpha \in \{A, C\}} z_\alpha^2 n_\alpha \cdot F'(R_\alpha, \lambda)}{\sum_{\alpha \in \{A, C\}} n_\alpha} \\ &= \frac{e_0^2}{4\pi(1+\chi)\varepsilon_0 k_B T} \frac{1}{8} \frac{\chi}{D} \Lambda \frac{\sum_{\alpha \in \{A, C\}} z_\alpha^2 n_\alpha \cdot F'(R_\alpha, \lambda)}{\sum_{\alpha \in \{A, C\}} n_\alpha}. \quad (122) \end{aligned}$$

For strong dilution, Δ_{sim} approaches Δ_{ideal} , $F'(R_\alpha, \lambda)$ converges for all R_α to the same value $F'_0 = 3$ and the neutral salt dissociates completely into ν_A anions and ν_C cations. We thus can write $n_\alpha = \nu_\alpha n^{\text{ref}} \cdot c$. Then, the definition of Λ according to (35) implies

$$\frac{\Delta_{\text{ideal}} - \Delta}{\Delta_{\text{ideal}}} = \frac{F'_0}{8} \frac{e_0^2}{4\pi(1+\chi)\varepsilon_0 k_B T} \frac{\chi}{D} \sqrt{\frac{e_0^2}{(1+\chi)\varepsilon_0 k_B T} \sum_{\alpha \in \{A, C\}} z_\alpha^2 \nu_\alpha \cdot c} \cdot \frac{\sum_{\alpha \in \{A, C\}} z_\alpha^2 \nu_\alpha}{\sum_{\alpha \in \{A, C\}} \nu_\alpha}. \quad (123)$$

We conclude, that in the strong dilution limit the same three theorems formulated in [DH23a] are also valid here, i.e. $(\Delta_{\text{ideal}} - \Delta)/\Delta_{\text{ideal}}$ is:

1. proportional to \sqrt{c} ,
2. proportional to $(\sum_{\alpha \in \{A, C\}} \nu_\alpha z_\alpha^2 / \sum_{\alpha \in \{A, C\}} \nu_\alpha)^{3/2}$,
3. proportional to $(1+\chi)^{-3/2}$.

Applying $\nu_A = \nu_C = 1$ and $F'_0 = 3$ to (123), we get for $c \rightarrow 0$ the approximation

$$\Delta/\Delta_{\text{ideal}} \approx 1 - S_\Delta \cdot \sqrt{2c} \quad \text{with the slope } S_\Delta = 0.5823. \quad (124)$$

This limit slope is more steep compared to the slope $S_\Delta^{\text{DH23}} = 0.2588$ that is obtained for the Debye-Hückel energy according to [DH23a] with $(F^{\text{DH23}})' \rightarrow 4/3$ for $c \rightarrow 0$, cf. the supporting material.

6 Discussion and conclusions

Failure of pure steric models. As shown in Sect. 4, the simple mixture, which serves as a representative of the class of sterically modified Poisson-Boltzmann models, cannot reproduce the apparent molar volume in aqueous solutions. Admittedly, this type of models were not developed with this goal in mind, but rather to limit charge accumulation in highly concentrated boundary layers. However, the main feature of these models is the introduction of a size parameter for the ions, and the most obvious way to identify this parameter should be the mass density of the solutions. Although fitting the model is in principle possible in the regime where sufficiently accurate experimental data can be found, two objections remain: i.) The simple mixture predicts a horizontal slope of $\Phi_V(\sqrt{c})$ at infinite dilution. ii.) The direct relationship of the apparent molar volume to the degree of dissociation necessarily requires that a considerable amount of undissociated ion pairs are already present in fairly dilute solutions of strong electrolytes, which seems unrealistic.

We thus find that the correct representation of the molar volume of electrolytes must take into account the electrical interaction of the ions, which the simple mixture cannot adequately do, since it treats all constituents as uncharged. On the other hand, there is no reason to exclude the simple mixture from the model, as it incorporates the mechanical and thermal properties of the electrolyte.

Simple mixture in coupled model. The coupling of the simple mixture model with another free energy contribution proposed here requires careful modifications of the axiomatic derivation procedure described in [BDD23]. Since in the coupling also the other contribution must in general also be expected to contribute to the total pressure, as is the case with the electric interaction energy derived above, the simple mixture model can not be built on an assumed law for the specific heat capacity at constant pressure. Instead, the derivation must be based on the specific heat capacity at constant volume. Another essential ingredient of the simple mixture model is the thermal equation of state, which relates the pressure contribution to the volume. It contains the bulk modulus, which in the case of water typically is large compared to the ambient pressure, leading to the notion of incompressibility. Although the incompressibility can not be exploited if the balancing of the different pressure contributions in the coupling is the focus of interest, the coupled system should also fulfill the requirement that the molar volume function $\nu^{\text{sim}}(T, \mathbf{y})$ in (26) depends linearly on the composition.

Ion interaction energy contribution. For the electric ion-ion interaction, we derived a free energy contribution that shares some simplifying assumptions with the derivation of Debye and Hückel. In particular, the local

perturbation of the free charge in the electrolyte caused by the ion is approximated on the microscopic level by a linearized Boltzmann distribution around the state in the far field. The local temperature T and number densities n_α from the macroscopic scale are used to define the far field $n_\alpha^\infty = n_\alpha$ and, consistent with the linearization, the spatially homogeneous temperature and susceptibility $\chi(T, (n_\alpha^\infty)_\alpha)$ on the microscopic scale. The linearization used in the derivation does not appear to be problematic due to the small amount of charge of the single selected ion. Likewise, on the microscopic scale, the concentration dependence of χ will have only minor impact due to the low charge accumulation in the boundary layer around the ion, whereas the dependence on the concentration is generally taken into account on the macroscopic scale.

The model uses solvated ion radii, which depend on temperature. This does not exclude the possibility that differently charged ions approach each other to form ion pairs. However, it makes it possible to take into account a reduction in volume during dissociation, as in LiF and NaF, without having to introduce e.g. holes or other additional species into the mixture model. We also use the value of the susceptibility in the solvation shell, which is assumed locally on the macroscopic scale, since no other value is obvious to us. The value χ_S^{ref} of the pure solvent is not suitable in the solvation shell because the solvent molecules there differ from the free ones in that they are bound and no longer freely orientable.

The free energy density due to the electric interaction is then determined directly based on the general thermodynamic relations of Sect. 2. In contrast to the standard Debye-Hückel energy, neither an integration of the thermodynamic relations with respect to temperature is required, nor is the thought experiment of the charging process required as an aid, but instead the general thermodynamic consistency conditions lead to a new restriction. The temperature dependence of the susceptibility can not be freely chosen, but is predetermined by the thermodynamic conditions! We are not aware of a similar compatibility condition in the existing literature.

Although the energy derived here differs from standard Debye-Hückel energy, it shares some structural properties. In particular, the resulting limit laws for infinite dilution coincide in qualitative way but yield different limit slopes. However, the experimental uncertainty in mass density measurements does not allow a decision what is the correct limit slope.

Non-constant susceptibility. Experiments with dilute solutions suggest a linear dependence of the susceptibility on the number densities at the reference temperature of the experiment. The thermodynamic consistency condition then prescribes in general a nonlinear dependence for temperatures different from the reference temperature. As can be seen in Sect. 3.6, the deviation from linearity is small enough to maintain consistency with a

linear dependence as model input even in alternative model approaches with a deviating reference temperature. In the limit of infinite dilution, the temperature dependence of the susceptibility is independent of the dissolved salt and is determined exclusively by the thermal expansion of the solvent.

Incomplete dissociation. The numerical experiments show that the electric ion interaction energy provides the coupled model with an alternative mechanism for non-constant apparent molar volume in addition to incomplete dissociation. We include incomplete dissociation in general into the coupled model, even for strong electrolytes such as aqueous NaCl solutions, and observe that when using identical parameters, the dissociation degree is considerably higher in the coupled model compared to the pure simple mixture. For a solution of 0.5 mol L^{-1} NaCl the coupled model yields a fraction of undissociated ion pairs less than 0.05.

In principle, one might suspect that the inclusion of incomplete dissociation in the model is an attempt to increase the degrees of freedom to facilitate the fit of the results to experimental data. However, we note that the model targets dilute solutions of strong electrolytes as well as concentrated solutions of weak electrolytes and no clearly defined point is apparent where incomplete dissociation would set in. Moreover, the additional free model parameters introduced by incomplete dissociation are themselves also tied to independent experiments such as the dielectric decrement.

More generally, in the material modeling we rely almost entirely on linear mixing laws that require only a minimal number of parameters. Linear laws are applied for the molar volume function $\nu^{\text{sim}}(T, \mathbf{y})$, specific heat $c_v(T, \nu^{\text{sim}}, \mathbf{y})$, specific internal energy $\bar{u}(T^{\text{ref}}, \nu^{\text{sim}}, \mathbf{y})$ and susceptibility $\chi(T^{\text{ref}}, (n_\alpha)_\alpha)$. Only the specific entropy $\bar{s}(T^{\text{ref}}, \nu^{\text{sim}}, \mathbf{y})$ contains an additional logarithmic contribution of Boltzmann type, but without adjustable parameters. Instead of modelling nonlinear material behaviour by adding nonlinear terms with additional parameters to the mentioned material laws, which in the case of ν^{sim} would even be incompatible with an incompressible limit, the nonlinearity in our model is realized by the dissociation reaction.

Numerical results. In the above numerical studies, the coupled model is successfully applied to reproduce the apparent molar volume over a wider range of salt concentration and temperature. From experiments with related salts that share either an anion or a cation, a consistent set of ion specific parameters can be deduced. Notably, for aqueous LiCl solutions of fixed salt concentration and varying temperature, the model predicts the local maximum of the apparent molar volume at $T \approx 40^\circ\text{C}$, much earlier than for solutions of NaCl or KCl. The solvated ion radii deduced here from mass density measurements are considerably smaller than those derived from steric Poisson-Boltzmann models applied to double layer capacitance

experiments, cf. e.g. [LGD16, LM22]. Independent experiments related to phase boundaries, such as vapour pressure reduction or freezing point depression confirm the previously identified model parameters. In terms of the 'osmotic coefficient' as a comparison measure, the numerical results show good agreement with available direct experimental data.

We remark that here no particular emphasis was placed on parameter optimization. An effort to tune model parameter for an optimal fit of experimental results should be based on more high precision experimental data.

Outlook. The model proposed here should next be applied to other the classical tests of electrolyte theory, such as the heat of dilution and the concentration dependent specific heat capacity c_p at fixed external pressure. However, such tests also require further input parameter related to the thermal properties of the electrolyte, i.e. the specific heat capacities c_α^{ref} which define $c_v(T, \nu^{\text{sim}}, \mathbf{y})$ (at fixed volume) but are unknown for the solvated ions. In addition, the model should be applied to electromotive force of Galvanic cells, which are used to evaluate activity coefficients as characteristic measures for electrolytes. This requires careful modeling of the involved electrode surface reactions in the way of [DGM16, DGM18].

In order to limit the scope of this paper, the applications and numerical studies here have been restricted to solutions of binary electrolytes of monovalent ions. For example, the autoprotolysis of water, possibly different solvation shells of ions depending on the salt input, or different types of ion pairs have been neglected here. The model can and should also be applied to solutions with multivalent ions whose description with the classical Debye-Hückel theory has weaknesses. However, the mere application of the above equations with only increased charge numbers may not be sufficient and careful consideration of the different dissociation steps and properties of the solvation shell of multivalent ions may be required.

The striking symmetry of the measured differential double layer capacitance of a non-adsorbing electrolyte such as KPF_6 on single crystal surfaces, cf. e.g. [Val81], suggests that in a steric Poisson-Boltzmann model $v_A^{\text{ref}} = v_C^{\text{ref}}$ and one could even be led to conjecture that the specific volume of an ion depends only on the solvation number κ_α , which in turn is determined solely by the valence of the ion. Taking the solvated ion radii deduced here from the apparent molar volume at infinite dilution as input parameters of the steric model, it would be interesting to analyze, whether or not the dependence of the susceptibility on the strong electric field inside the double layer, cf. e.g. [BKSA09, LM22], instead of the elastic volume exclusion effects, can explain the experimentally observed symmetry of the double layer capacitance.

References

- [AM99] A. Apelblat and E. Manzurola. Volumetric properties of water, and solutions of sodium chloride and potassium chloride at temperatures from $T = 277.15K$ to $T = 343.15K$ at molalities of (0.1, 0.5, and 1.0) $mol \cdot kg^{-1}$. *J. Chem. Thermodyn.*, 31(7):869–893, 1999.
- [AM01] A. Apelblat and E. Manzurola. Volumetric properties of aqueous solutions of lithium chloride at temperatures from 278.15K to 338.15K and molalities (0.1, 0.5, and 1.0) $mol \cdot kg^{-1}$. *J. Chem. Thermodyn.*, 33(9):1133–1155, 2001.
- [Arr87] S. Arrhenius. Über die Dissociation der in Wasser gelösten Stoffe. *Z. Physik. Chem.*, 1:631–648, 1887.
- [AW81] G. C. Allred and E. M. Woolley. Heat capacities of aqueous *HCl*, *NaOH*, and *NaCl* at 283.15, 298.15 and 313.15 K: ΔC_p° for ionization of water. *J. Chem. Thermodyn.*, 13(2):147–154, 1981.
- [BAO97] I. Borukhov, D. Andelman, and H. Orland. Steric effects in electrolytes: A modified Poisson–Boltzmann equation. *Phys. Rev. Lett.*, 79:435–438, 1997.
- [BDD23] D. Bothe, W. Dreyer, and P.-E. Druet. Multicomponent incompressible fluids—An asymptotic study. *J. Appl. Math. Mech.*, 103(7):e202100174, 2023.
- [BHM99] R. Buchner, G. T. Hefter, and P. M. May. Dielectric relaxation of aqueous NaCl solutions. *J. Phys. Chem. A*, 103(1):1–9, 1999.
- [Bje26] N. Bjerrum. Untersuchungen über Ionenassoziation. *K. Dan. Vidensk. Selsk.*, 7(9), 1926.
- [BKSA09] M.Z. Bazant, M.S. Kilic, B.D. Storey, and A. Ajdari. Towards an understanding of induced-charge electrokinetics at large applied voltages in concentrated solutions. *Advances in Colloid and Interface Science*, 152(1-2):48 – 88, 2009.
- [BYAP11] D. Ben-Yaakov, D. Andelman, and R. Podgornik. Dielectric decrement as a source of ion-specific effects. *J. Chem. Phys.*, 134(7):074705, 2011.
- [CBL⁺07] V. B. Chu, Y. Bai, J. Lipfert, D. Herschlag, and S. Doniach. Evaluation of ion binding to dna duplexes using a size-modified poisson-boltzmann theory. *Biophys. J.*, 93(9):3202 – 3209, 2007.

- [CCM80] C.-T. A. Chen, J. H. Chen, and F. J. Millero. Densities of $NaCl$, $MaCl_2$, Na_2SO_4 , and $MgSO_4$ aqueous solutions at $1atm$ from 0 to $50^\circ C$ and from 0.001 to 1.5m. *J. Chem. Eng. Data*, 25(4):307–310, 1980.
- [CG85] E. C. W. Colin and D. N. Glew. Evaluation of the thermodynamic functions for aqueous sodium chloride from equilibrium and calorimetric measurements below $154^\circ C$. *J. Phys. Chem. Ref. Data*, 14(2):489–610, 1985.
- [CHB03] T. Chen, G. Heftler, and R. Buchner. Dielectric spectroscopy of aqueous solutions of KCl and $CsCl$. *J. Phys. Chem. A*, 107(20):4025–4031, 2003.
- [Deb24] P. Debye. Osmotische Zustandsgleichung und Aktivität verdünnter starker Elektrolyte. *Physik. Z.*, 25:97–107, 1924.
- [dGM84] S. R. de Groot and P. Mazur. *Non-equilibrium Thermodynamics*. Dover Publications, New York, 1984.
- [DGM13] W. Dreyer, C. Guhlke, and R. Müller. Overcoming the shortcomings of the Nernst–Planck model. *Phys. Chem. Chem. Phys.*, 15:7075–7086, 2013.
- [DGM16] W. Dreyer, C. Guhlke, and R. Müller. A new perspective on the electron transfer: recovering the Butler-Volmer equation in non-equilibrium thermodynamics. *Phys. Chem. Chem. Phys.*, 18:24966–24983, 2016.
- [DGM18] W. Dreyer, C. Guhlke, and R. Müller. Bulk-surface electrothermodynamics and applications to electrochemistry. *Entropy*, 20(12):939, 2018.
- [DGM19] W. Dreyer, C. Guhlke, and R. Müller. The impact of solvation and dissociation on the transport parameters of liquid electrolytes: continuum modeling and numerical study. *Eur. Phys. J.-Spec. Top.*, 227(18):2515–2538, 2019.
- [DH23a] P. Debye and E. Hückel. Zur Theorie der Elektrolyte I. Gefrierpunktserniedrigung und verwandte Erscheinungen. *Physik. Z.*, 24(9):185–206, 1923.
- [DH23b] P. Debye and E. Hückel. Zur Theorie der Elektrolyte II. Das Grenzgesetz für die elektrische Leitfähigkeit. *Physik. Z.*, 24:305–325, 1923.
- [Ell66] A. J. Ellis. Partial molal volumes of alkali chlorides in aqueous solution to 200° . *J. Chem. Soc. A*, pages 1579–1584, 1966.

- [FCBM16] B. Figliuzzi, W.H.R. Chan, C.R. Buie, and J.L. Moran. Nonlinear electrophoresis in the presence of dielectric decrement. *Phys. Rev. E*, 94:023115, Aug 2016.
- [GG74] H. F. Gibbard and A. F. Gossmann. Freezing points of electrolyte mixtures. I. mixtures of sodium chloride and magnesium chloride in water. *J. Solution Chem.*, 3(5):385–393, 1974.
- [GH25] P. Groß and O. Halpern. Über die temperaturabhängigen Parameter in der Statistik und die Debyesche Elektrolyttheorie. *Physik. Z.*, 26:403–407, 1925.
- [GS18] A. Gupta and H.A. Stone. Electrical double layers: Effects of asymmetry in electrolyte valence on steric effects, dielectric decrement, and ion–ion correlations. *Langmuir*, 34(40):11971–11985, 2018.
- [GW85] J. A. Gates and R. H. Wood. Densities of aqueous solutions of sodium chloride, magnesium chloride, potassium chloride, sodium bromide, lithium chloride, and calcium chloride from 0.05 to 5.0 mol · kg⁻¹ and 0.1013 to 40MPa at 298.15K. *J. Chem. Eng. Data*, 30(1):44–49, 1985.
- [Hey96] R. Heyrovská. Physical electrochemistry of strong electrolytes based on partial dissociation and hydration: Quantitative interpretation of the thermodynamic properties of NaCl(aq) from “zero to saturation”. *J. Electrochem. Soc.*, 143(6):1789–1793, jun 1996.
- [HGBS95] N. Hubert, Y. Gabes, J.-B. Bourdet, and L. Schuffenecker. Vapor pressure measurements with a nonisothermal static method between 293.15 and 363.15 K for electrolyte solutions. application to the H₂O + NaCl system. *J. Chem. Engin. Data*, 40(4):891–894, 1995.
- [HH21] L. Hnedkovsky and G. Hefter. Densities and apparent molar volumes of aqueous solutions of NaClO₄, KClO₄, and KCl at temperatures from 293 to 343 K. *J. Chem. Eng. Data*, 66(9):3645–3658, 2021.
- [HHLH16] B. Hu, L. Hnedkovsky, W. Li, and G. Hefter. Densities and molar volumes of aqueous solutions of LiClO₄ at temperatures from 293 K to 343 K. *J. Chem. Eng. Data*, 61(4):1388–1394, 2016.
- [HO59] H.S. Harned and B.B. Owen. *The Physical Chemistry of Electrolytic Solutions*. Reinhold, New York, third edition, 1959.

- [HRC48] J. B. Hasted, D. M. Ritson, and C. H. Collie. Dielectric properties of aqueous ionic solutions. parts I and II. *J. Chem. Phys.*, 16(1):1–21, 1948.
- [HSB88] D. L. Hall, S. M. Sterner, and R. J. Bodnar. Freezing point depression of *NaCl-KCl-H₂O* solutions. *Econ. Geol.*, 83(1):197–202, 1988.
- [Hüc25] E. Hückel. Zur Theorie konzentrierterer wässriger Lösungen starker Elektrolyte. *Physik. Z.*, 26:93–147, 1925.
- [HvRL12] M.M. Hatlo, R. van Roij, and L. Lue. The electric double layer at high surface potentials: The influence of excess ion polarizability. *EPL*, 97(2):28010, Jan 2012.
- [HW72] W. J. Hamer and Y.-C. Wu. Osmotic coefficients and mean activity coefficients of uni-univalent electrolytes in water at 25°C. *J. Phys. Chem. Ref. Data*, 1(4):1047–1100, 1972.
- [KBA07] M. S. Kilic, M. Z. Bazant, and A. Ajdari. Steric effects in the dynamics of electrolytes at large applied voltages. I. Double-layer charging. *Phys. Rev. E*, 75:021502, 2007.
- [KII96] V. Kralj-Iglič and A. Iglič. A simple statistical mechanical approach to the free energy of the electric double layer including the excluded volume effect. *J. Phys. II*, 6(4):477–491, 1996.
- [KMMT18] G. M. Kontogeorgis, B. Maribo-Mogensen, and K. Thomsen. The Debye-Hückel theory and its importance in modeling electrolyte solutions. *Fluid Ph. Equilib.*, 462:130–152, 2018.
- [LE14] J.-L. Liu and B. Eisenberg. Poisson-Nernst-Planck-Fermi theory for modeling biological ion channels. *J. Chem. Phys.*, 141(22):22D532, 2014.
- [LE15] J.-L. Liu and B. Eisenberg. Poisson-Fermi model of single ion activities in aqueous solutions. *Chem. Phys. Lett.*, 637:1–6, 2015.
- [LE18] J.-L. Liu and B. Eisenberg. Poisson-Fermi modeling of ion activities in aqueous single and mixed electrolyte solutions at variable temperature. *J. Chem. Phys.*, 148(5):054501, 02 2018.
- [LGD16] M. Landstorfer, C. Gohlke, and W. Dreyer. Theory and structure of the metal-electrolyte interface incorporating adsorption and solvation effects. *Electrochim. Acta*, 201:187–219, 2016.
- [Li09] B. Li. Continuum electrostatics for ionic solutions with non-uniform ionic sizes. *Nonlinearity*, 22(4):811–833, feb 2009.

- [Lid05] D.P. Lide, editor. *CRC Handbook of Chemistry and Physics*. CRC PRESS, 2005.
- [LM29] E. Lange and J. Meixner. Zur Individualität der integralen Verdünnungswärmen starker Elektrolyte. *Physik. Z.*, 30:670–678, 1929.
- [LM22] M. Landstorfer and R. Müller. Thermodynamic models for a concentration and electric field dependent susceptibility in liquid electrolytes. *Electrochim. Acta*, 428:140368, 2022.
- [Mar11] Y. Marcus. Electrostriction in electrolyte solutions. *Chem. Rev.*, 111(4):2761–2783, 2011.
- [Mar13] Y. Marcus. Evaluation of the static permittivity of aqueous electrolytes. *J. Solution Chem.*, 42(12):2354–2363, 2013.
- [Mas29] D. O. Masson. Solute molecular volumes in relation to solvation and ionization. *Philos. Mag.*, 8(49):218–235, 1929.
- [MDH68] F. J. Millero and W. Drost-Hansen. Apparent molal volumes of aqueous monovalent salt solutions at various temperatures. *J. Chem. Eng. Data*, 13(3):330–333, 1968.
- [MH06] Y. Marcus and G. Hefter. Ion pairing. *Chem. Rev.*, 106(11):4585–4621, 2006.
- [Mil71] F. J. Millero. Molal volumes of electrolytes. *Chem. Rev.*, 71(2):147–176, 1971.
- [ML23] R. Müller and M. Landstorfer. Galilean bulk-surface electrothermodynamics and applications to electrochemistry. *Entropy*, 25(3):416, 2023.
- [MR17] P. M. May and D. Rowland. Thermodynamic modeling of aqueous electrolyte systems: Current status. *J. Chem. Engin. Data*, 62(9):2481–2495, 2017.
- [Mül85] I. Müller. *Thermodynamics*. Pitman Publishing, London, 1985.
- [NA15] Y. Nakayama and D. Andelman. Differential capacitance of the electric double layer: The interplay between ion finite size and dielectric decrement. *J. Chem. Phys.*, 142(4):044706, 2015.
- [Ons27] L. Onsager. Zur Theorie der Elektrolyte II. *Physik. Z.*, 28(8):277–298, 1927.
- [PD72] C. N. Pepela and P. J. Dunlop. A re-examination of the vapour pressures of aqueous sodium chloride solutions at 25 °C. *J. Chem. Thermodyn.*, 4(2):255–258, 1972.

- [PDH84] T. G. Pedersen, C. Dethlefsen, and A. Hvidt. Volumetric properties of aqueous solutions of alkali halides. *Carlsberg Res. Commun.*, 49(3):445–455, 1984.
- [PG08] R. H. Perry and D. W. Green, editors. *Perry’s chemical engineers’ handbook*. McGraw-Hill, New York, 8 edition, 2008.
- [Red46] O. Redlich. The dissociation of strong electrolytes. *Chem. Rev.*, 39(2):333–356, 1946.
- [RM64] O. Redlich and D. M. Meyer. The molal volumes of electrolytes. *Chem. Rev.*, 64(3):221–227, 1964.
- [RR31] O. Redlich and P. Rosenfeld. Das partielle molare Volumen von gelösten Elektrolyten. I. *Z. Phys. Chem.*, 155A(1):65–74, 1931.
- [RS02] R.A. Robinson and R.H. Stokes. *Electrolyte Solutions*. Dover Publications, New York, second revised edition, 2002.
- [SL15] I. Y. Shilov and A. K. Lyashchenko. The role of concentration dependent static permittivity of electrolyte solutions in the Debye–Hückel theory. *J. Phys. Chem. B*, 119(31):10087–10095, 2015.
- [SLK23] G. M. Silva, X. Liang, and G. M. Kontogeorgis. How to account for the concentration dependency of relative permittivity in the Debye–Hückel and Born equations. *Fluid Ph. Equilib.*, 566:113671, 2023.
- [Val81] G. Valette. Double layer on silver single-crystal electrodes in contact with electrolytes having anions which present a slight specific adsorption: Part I. the (110) face. *J. Electroanal. Chem.*, 122:285–297, 1981.
- [VB14] M. Valiskó and D. Boda. The effect of concentration- and temperature-dependent dielectric constant on the activity coefficient of NaCl electrolyte solutions. *J. Chem. Phys.*, 140(23):234508, 2014.
- [VB23] M. Valiskó and D. Boda. Resurrection of Hückel’s idea: Decoupling ion–ion and ion–water terms in activity coefficients via the state-dependent dielectric constant. *Fluid Ph. Equilib.*, 572:113826, 2023.
- [VVB10] J. Vincze, M. Valiskó, and D. Boda. The nonmonotonic concentration dependence of the mean activity coefficient of electrolytes is a result of a balance between solvation and ion-ion correlations. *J. Chem Phys*, 133(15):154507, 10 2010.

- [Zav01] A. A. Zavitsas. Properties of water solutions of electrolytes and nonelectrolytes. *J. Phys. Chem. B*, 105(32):7805–7817, 2001.
- [ZH18] Y. Zhang and J. Huang. Treatment of ion-size asymmetry in lattice-gas models for electrical double layer. *J. Phys. Chem. C*, 122(50):28652–28664, 2018.